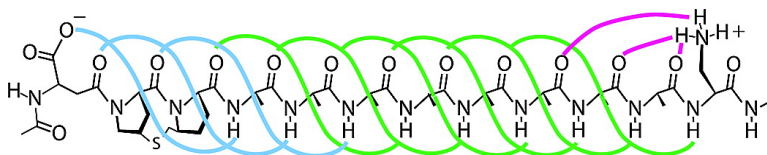


Water-Solubilized, Cap-Stabilized, Helical Polyalanines: Calibration Standards for NMR and CD Analyses

Bjrn Heitmann, Gabriel E. Job, Robert J. Kennedy, Sharon M. Walker, and Daniel S. Kemp

J. Am. Chem. Soc., **2005**, 127 (6), 1690-1704 • DOI: 10.1021/ja0457462 • Publication Date (Web): 22 January 2005

Downloaded from <http://pubs.acs.org> on March 24, 2009



More About This Article

Additional resources and features associated with this article are available within the HTML version:

- Supporting Information
- Links to the 9 articles that cite this article, as of the time of this article download
- Access to high resolution figures
- Links to articles and content related to this article
- Copyright permission to reproduce figures and/or text from this article

[View the Full Text HTML](#)

Water-Solubilized, Cap-Stabilized, Helical Polyalanines: Calibration Standards for NMR and CD Analyses

Björn Heitmann, Gabriel E. Job, Robert J. Kennedy, Sharon M. Walker, and Daniel S. Kemp*

Contribution from the Department of Chemistry, Room 18-296, Massachusetts Institute of Technology, Cambridge, Massachusetts 02139

Received July 15, 2004; E-mail: kemp@mit.edu

Abstract: NMR and CD studies are reported for two length series of solubilized, spaced, highly helical polyalanines that are N-capped by the optimal helix stabilizer β Asp-Hel and C-capped by β -aminoalanine *beta* and that are studied in water at 2 °C, pH 1–8. NMR analysis yields a structural characterization of the peptide $\text{Ac}\beta\text{AspHelAla}_8\text{betaNH}_2$ and selected members of one $\beta\text{AspHelAla}_n\text{beta}$ series. At pH > 4.5 the βAspHel cap provides a preorganized triad of carboxylate anion and two amide residues that is complementary to the helical polyalanine N-terminus. The C-terminal β -aminoalanine assumes a helix-stabilizing conformation consistent with literature precedents. H(N)CO NMR experiments applied to capped, uniformly ^{13}C - and ^{15}N -labeled Ala_8 and Ala_{12} peptides define Ala_n hydrogen bonding signatures as α -helical without detectable 3_{10} character. Relative $\text{NH}\rightarrow\text{ND}$ exchange rates yield site protection factors PF_i that define uniquely high fractional helicities FH for the peptide Ala_n regions. These Ala_n calibration series, studied in water and lacking helix-stabilizing tertiary structure, yield the first ^{13}C NMR chemical shifts, $^3J_{\text{HNH}\alpha}$ coupling constants, and CD ellipticities $[\theta_{\text{Molar}}]_{\lambda,n}$ characteristic of a fully helical alanine within an Ala_n context. CD data are used to assign parameters X and $[\theta]_{\lambda,\infty}$, required for rigorous calculation of FH values from CD ellipticities.

Introduction

Alanine is the simplest strongly helix-forming α -amino acid, and polyalanines are natural choices for modeling helical structure and energetics.¹ Bio-relevant tests of modeling predictions require helicity data for fully helical Ala_n peptides in aqueous solution. A definitive X-ray fiber diffraction structure of helical polyalanine in the solid state was reported nearly forty years ago,² but up to now, comparable structural studies in water have been unavailable. Low Ala_n solubilities and high aggregation have long been addressed by triblock constructs that flank central polyalanines by solubilizing N- and C-terminal peptide caps.³

As well as inhibiting formation of Ala_n β -sheet aggregates,⁴ an ideal pair of caps must suppress extension of the helix beyond the boundaries of the Ala_n region as well as interactions of charged solubilizers with the helix. Heteropeptide constructs shown in Figure 1a⁵ solve these problems and allow analysis of intrinsic properties of simple helical Ala_n peptides, $6 \leq n \leq$

45, in water, but these lack conformational homogeneity. Fractional helicities⁶ FH for the Ala_n region are substantially less than 1.0,⁵ since the completely helical conformation equilibrates with nonhelical and partially helical conformations of comparable stability.⁷ In the first part of this report we characterize the first water-soluble, maximally helical Ala_n length series and use it to assign structure and fundamental NMR parameters for hydrated, α -helical alanines.

How is maximal helicity achieved? Our research strategy was defined by Lifson–Roig modeling.⁸ If a homopeptide derived from a residue with a high helical propensity is N- and C-capped by strong helix stabilizers, the completely helical conformation is selectively stabilized and can dominate the manifold. The peptide $\text{Ac}\beta\text{AspHel-Ala}_8\text{-beta-NH}_2$, with the N-cap $\beta\text{Asp-Hel}^9$ and the C-cap β -aminoalanine $\equiv \text{beta}$,¹⁰ was previously shown from $\text{NH}\rightarrow\text{ND}$ exchange-derived site protection factors PF_i ¹¹

- (1) (a) Wiczcerek, R.; Dannenberg, J. J. *J. Am. Chem. Soc.* **2003**, *125*, 8124–8129. (b) Mahadevan, J.; Lee, K.-H.; Kuczera, K. *J. Phys. Chem. B* **2001**, *105*, 1863–1876. (c) Levy, Y.; Jortner, J.; Becker, O. M. *Proc. Natl. Acad. Sci. U.S.A.* **2001**, *98*, 2188–2193. (d) Lee, S.-H.; Krimm, S. *Biopolymers* **1998**, *46*, 283–317.
- (2) Arnott, S.; Dover, S. D. *J. Mol. Biol.* **1967**, *30*, 209–212.
- (3) (a) Gratzner, W. B.; Doty, P. *J. Am. Chem. Soc.* **1963**, *85*, 1193–1197. (b) Ingwall, R. T.; Scheraga, H. A.; Lotan, N.; Berger, A.; Katchalski, E. *Biopolymers* **1968**, *6*, 331–368.
- (4) (a) Forood, B.; Pérez-Payá, E.; Houghten, R. A. *Blondelle, S. E. Biochem. Biophys. Res. Commun.* **1995**, *211*, 7–13. (b) Blondelle, S. E.; Forood, B.; Houghten, R. A.; Pérez-Payá, E. *Biochemistry* **1997**, *36*, 8393–8400.

- (5) (a) Miller, J. S.; Kennedy, R. J.; Kemp, D. S. *Biochemistry* **2001**, *40*, 305–309. (b) Miller, J. S.; Kennedy, R. J.; Kemp, D. S. *J. Am. Chem. Soc.* **2002**, *124*, 945–962. (c) Kennedy, R. J.; Tsang, K.-Y.; Kemp, D. S. *J. Am. Chem. Soc.* **2002**, *124*, 934–944.
- (6) For each peptide under particular experimental conditions, FH is defined as the ratio of helical α -carbons to all Ala_n α -carbons; its range is 0 to 1. Owing to charge repulsion, Lys_m regions are nonhelical.
- (7) (a) Zimm, B. H.; Bragg, J. K. *J. Chem. Phys.* **1959**, *31*, 526–535. (b) Zimm, B. H.; Doty, P. *Proc. Natl. Acad. Sci. U.S.A.* **1959**, *45*, 1601–1607. (c) Lifson, S.; Roig, A. *J. Chem. Phys.* **1961**, *34*, 1963–1974.
- (8) Kemp, D. S. *Helv. Chim. Acta* **2002**, *85*, 4392–4423.
- (9) Maison, W.; Arce, E.; Renold, P.; Kennedy, R. J.; Kemp, D. S. *J. Am. Chem. Soc.* **2001**, *123*, 10245–10254.
- (10) Deechongkit, S.; Tsang, K.-L.; Renold, P.; Kennedy, R. J.; Kemp, D. S. *Tetrahedron Lett.* **2000**, *41*, 9679–9683.
- (11) Bai, Y.; Milne, J. S.; Mayne, L.; Englander, S. W. *Proteins: Struct., Funct., Genet.* **1993**, *17*, 75–86.

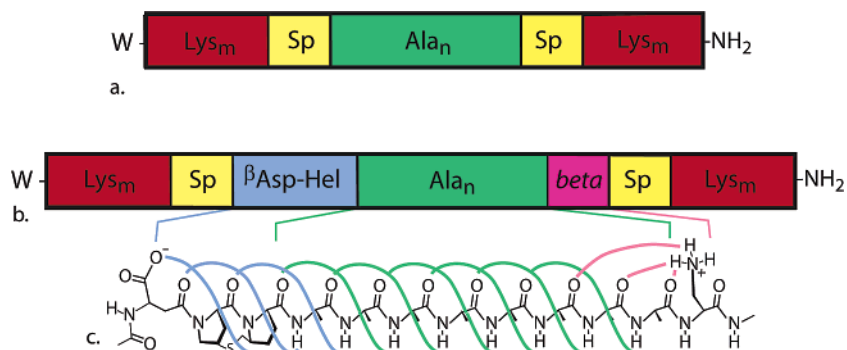


Figure 1. (a, b) Schematics depicting peptide sequences for spaced, solubilized polyalanines. (a) Color code: red, solubilizing polylysine regions; yellow, spacers that confine helical structure to the green Ala_n region and isolate it from interactions with the charged Lys_m regions. (b) Added are the helix-stabilizing N-capping regions βAspHel, blue, and the helix-stabilizing and terminating C-cap, beta ≡ β-aminoalanine, purple. Spacing elements Sp include combinations of ^tL-*tert*-leucine, Inp ≡ 4-carboxypiperidine; Acc ≡ *trans*-4-aminocyclohexanecarboxylic acid. (c) Depiction of the helical hydrogen bonding connectivity of the βAspHel-Ala_n-beta sequence, as demonstrated in this report.

to have a FH ≃ 0.95.^{5c} In this report we generalize this result to members of βAspHel-Ala_n-beta length series, characterizing their Ala_n region FH values by NH → ND exchange. These provide a hitherto missing calibration for CD-based FH assignments.^{5b,12}

This study is timely. It introduces model systems that may be used to confirm predictions of recent polyalanine modeling experiments;¹ it takes a key step toward improving the accuracy and precision of CD-based helicity assignments;¹³ and it may provide insight into sequences and experimental conditions that predispose or inhibit sheet or helix formation by polyalanine peptide sequences of current relevance to materials science¹⁴ and to medicine.¹⁵

An Overview of NMR and CD Structural Issues

A key question underlies both NMR and CD studies. Do the N- and C-caps of the βAspHel-Ala_n-beta series selectively enhance the mole fractions of the completely helical Ala_n conformations without globally distorting their structures? In other words, can one treat the capping effect as a structural perturbation, confined to terminal regions? The intrinsic structure of an α-helix renders cap-initiated global distortions implausible. The helical backbone defines a cylinder of fixed diameter, and all its intramolecular hydrogen bonds, van der Waals contacts, and nonpolar interactions occur locally, between pairs of residues belonging to contiguous three-residue loops. For *n* larger than an experimentally assigned minimum length, and for an ideal fully hydrated Ala_n helix, the properties of core residues that are isolated from the terminal regions should converge to limiting cap-independent values. This principle underlies CD-based quantitation of FH¹⁶ that relies on the

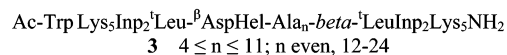
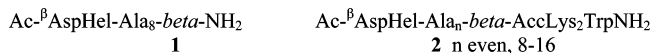
familiar eq 1. In subsequent sections, we use NMR and CD data to assign this minimum length.

$$[\theta]_{\lambda,n} = [\theta]_{\lambda,\infty} (1 - X/n) = [\theta]_{\lambda,\infty} - [\theta]_{\lambda,\infty} (X/n) \quad (1)$$

$[\theta]_{\lambda,n}$ is the molar per residue ellipticity at λ nm of a peptide of length *n* with FH 1.0; *X*, with dimensions of length in residues, corrects for capping effects; $[\theta]_{\lambda,\infty}$ is the convergent core ellipticity

Design of N- and C-Capped Peptides Containing a Central Sequence βAspHel-Ala_n-beta for NMR and CD Spectroscopic Roles: Peptide 1 and the Peptide Series 2 and 3

NMR and CD experiments require different βAspHel-Ala_n-beta peptide series. The CD series must span a large range of *n*, and the lengths of the Lys_m caps must be sufficient to inhibit aggregation. NMR structural studies require spectra that are dominated by Ala resonances, with minimal ¹H, ¹³C, and ¹⁵N resonance overlaps. The initial NMR structural assignments employed the previously studied Ala₈ peptide **1**, which lacks solubilizing regions.^{5c}



Peptides of series **3** were designed to meet the needs of CD calibrations.⁵ The Trp residue, which is isolated from the helical region, was required for accurate concentration determination, and the ten Lys residues were chosen from previous studies.^{5b} Although PF_{*i*} measurements and other NMR characterization experiments were carried out on representative members of this series, assignments of ³J_{H_{NH}α} coupling constants and residue-specific PF_{*i*} values were complicated by anomalous splitting and broadening of Ala NH resonances, attributable to the Inp spacers. Inp itself is achiral, but its simple N-acyl derivatives contain a chiral center, Figure 2, and the corresponding series **3** peptides, which contain a pair of Inp₂ functions, are diastereomeric mixtures. The expected NH peak widths and multiplicities are restored if Inp₂ is replaced in series **2** by a single achiral Acc spacing element derived from *trans*-4-aminocyclohexanecarboxylic acid. This series, patterned on structure **1**, was

- (12) (a) Wallimann, P.; Kennedy, R. J.; Kemp, D. S. *Angew. Chem., Int. Ed.* **1999**, *38*, 1290–1292. (b) Wallimann, P.; Kennedy, R. J.; Miller, J. S.; Shalongo, W.; Kemp, D. S. *J. Am. Chem. Soc.* **2003**, *125*, 1203–1220.
(13) (a) Chakrabarty, A.; Kortemme, T.; Baldwin, R. L. *Protein Sci.* **1994**, *3*, 843–852. (b) Park, S. H.; Shalongo, W.; Stellwagen, E. *Biochemistry* **1993**, *32*, 7038–7053. (c) Myers, J. K.; Pace, C. N.; Scholtz, J. M. *Biochemistry* **1997**, *36*, 10923–10929.
(14) (a) Nakazawa, Y.; Asakura, T. Y. *Macromolecules* **2002**, *35*, 2393–2400. (b) Rathore, O.; Sogah, D. Y. *J. Am. Chem. Soc.* **2001**, *123*, 5231–5239.
(15) (a) Baxter, S. W.; Choong, D. Y. H.; Eccles, D. M.; Campbell, I. G. *Cancer Epidemiol., Biomarkers Prev.* **2002**, *11*, 211–214. (b) Bruneau, S.; Johnson, K. R.; Yamamoto, M.; Kuroiwa, A.; Duboule, D. *Dev. Biol.* **2001**, *237*, 345–353. (c) Perutz, M.; Pope, B. J.; Owen, D.; Wanker, E. E.; Scherzinger, E. *Proc. Natl. Acad. Sci. U.S.A.* **2002**, *99*, 5596–5600.
(16) (a) Chen, Y.-H.; Yang, J. T.; Martinez, H. M. *Biochemistry* **1972**, *11*, 4120–4131. (b) Woody, R. W.; Tinoco, I., Jr. *J. Chem. Phys.* **1967**, *46*, 4927–4945. (c) Johnson, W. C., Jr.; Tinoco, I., Jr. *J. Am. Chem. Soc.* **1972**, *94*, 4389–4390.

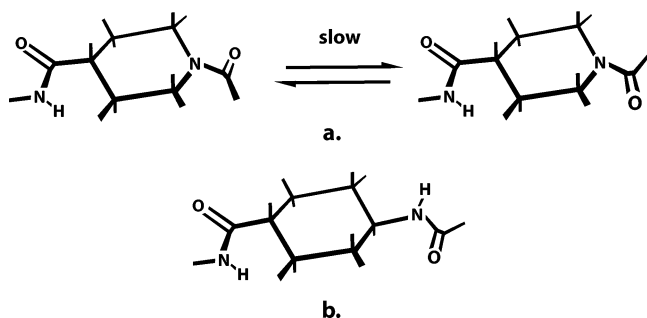


Figure 2. (a) Depiction of a pair of isoenergetic mirror image *N*-acyl-Inp functions; owing to amide resonance, these are in slow equilibrium on the NMR time scale at ambient temperatures. A pair of diastereomers is generated by each Inp function, accounting for the multiplicities and line broadening observed for Ala_{*n*} ¹H NH resonances of series 3 peptides. (b) Depiction of the achiral, rigid Acc used as a spacing element for series 2 peptides. Derived from *trans*-4-aminocyclohexane carboxylic acid, this element joins peptide regions by secondary amide bonds that assume the *s*-*trans* conformation. Modeling estimates the Acc distance between its 1-C=O and 4-NH atoms as 6.7 Å.

designed for both CD and NMR studies. To avoid aggregation we fixed the upper length limit for series 2 peptides at 16. For pairs of members of series 2 and 3 with identical Ala_{*n*} regions, cap-corrected CD spectra are equivalent within measurement error, as are FH values calculated from PF₁ measurements.

Application of AUC under CD and NMR measurement conditions to selected peptides that span the full length range of series 2 and 3 demonstrated absence of detectable aggregation.¹⁷ A preliminary test of NH → ND exchange rates in D₂O revealed that all non-Ala NH resonances exchange at rates expected for solvent-exposed protons. This result implies that hydrogen-bonded or solvent-shielded NH functions appear solely within the Ala_{*n*} regions for peptides of each series.

A brief review of helical structure introduces the next section which presents NMR evidence for cap conformations and interactions characteristic of βAspHel-Ala_{*n*}-β₂ peptides. An α-helix, Figure 1c, is spanned by three chains of successively hydrogen-bonded amides. A central helical amide at sites *i* and (*i* + 1) forms a donor H-bond to the amide CO of site (*i* - 3) and an acceptor H-bond to the amide NH of site (*i* + 4). Each of the three amides at the two helix ends forms only one intrahelical H-bond and carries an unsatisfied H-bonding valence. At each terminus, local amide dipoles sum to an experimentally demonstrable partial charge, positive at the N-terminus, negative at the C-terminus.¹⁸ Native structures of globular proteins often contain side chain functions that terminate helices by providing stabilizing terminal charges as well as missing hydrogen bond donors or acceptors.¹⁹ Helix stabilizing N- and C-caps are designed to incorporate these features.

The βAspHel N-cap provides an anion that can stabilize the local N-terminal helical dipole and act as an H-bond acceptor. The anion and two more H-bonding amides are preorganized to match orientations of the N-terminal helical NHs, Figure 1c.⁹ The C-cap β₂ provides an oriented positive charge, which may

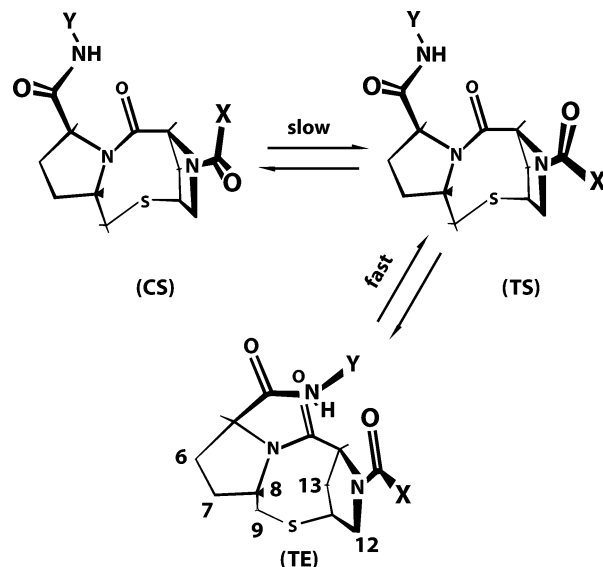


Figure 3. Three conformational states of a peptide conjugate of the *N*-acyl-Hel N-cap. On the NMR time scale in water at 2 °C, the (ts) and (te) states equilibrate and appear as a single set of resonances; owing to slow (c)–(t) amide rotation, the (cs) and composite (ts) + (te) states appear as distinct resonances. The (te) state stabilizes the helix, but the (cs) and (ts) states do not. For the highly helical peptides of this report, the (te) conformation is dominant.^{5c}

also form one or more strong hydrogen bonds to the three helical C-terminal carbonyl oxygens.¹⁰

Capping Region NMR Assignments for Peptides 1 and 2; Conformations and Interactions with the Ala₈ Region for βAspHel and β₂; Helical Stabilization by an Ionized βAsp Function

Initial 600 MHz NMR structural studies were carried out on peptide 1, Ac-βAspHel-Ala₈-β₂-NH₂, in aqueous solution at 2 °C, pH 3. Analysis of a ¹H NMR spectrum together with TOCSY and ROESY spectra allowed assignment of all ¹H resonances; no evidence for tertiary structure was detected. The major conformer was assigned a (t)-state structure, analogous to that previously characterized for Ac-Hel-peptide conjugates, Figure 3.²⁰ The spectra show eight resolved alanine NH resonances, linked by a continuous ladder of N,N(*i*, *i* + 1) cross-peaks. The Ala-1 resonance was assigned by cross-peaks that tie it to single Ala and to the Hel function. The NH resonance assigned to Ala-8 showed a pair of (*i*, *i* + 1) cross-peaks with the NH resonance of Ala-7 and with the backbone NH of β₂; the latter in turn showed an (*i*, *i* + 1) cross-peak with one of the two resonances of the C-terminal NH₂. These are consistent with the expected Ala₈ helical structure, terminated by the N- and C-caps.

A left-handed helical conformation is assigned for β₂, Figure 4a, from a pair of cross-peaks between the resonance corresponding to the α-proton of Ala-6 and both the α and one of the β-protons of β₂, together with a cross-peak between one of the C-terminal NH₂ protons and the β-proton of Ala-8. Similar conformations are reported for α-helix C-termination by Nagarajaram et al. from analysis of Asn and Gly examples from the protein X-ray crystallographic database.²¹

(17) Although the series 2 peptides (*n* ≤ 16) are unaggregated, longer members of this series have not been studied, and the aggregation-free upper limit of *n* for this series at millimolar concentrations in water is currently unknown.

(18) Tidor, B. *Proteins: Struct., Funct., Genet.* **1994**, *19*, 310–323.

(19) Aurora, R.; Rose, G. D. *Protein Sci.* **1998**, *7*, 21–38.

(20) Kemp, D. S.; Allen, T. J.; Oslick, S. L. *J. Am. Chem. Soc.* **1995**, *117*, 6641–6657.

(21) Nagarajaram, H. A.; Sowdhamini, R.; Ramakrishnan, C.; Balaram, P. *FEBS Lett.* **1993**, *321*, 79–83.

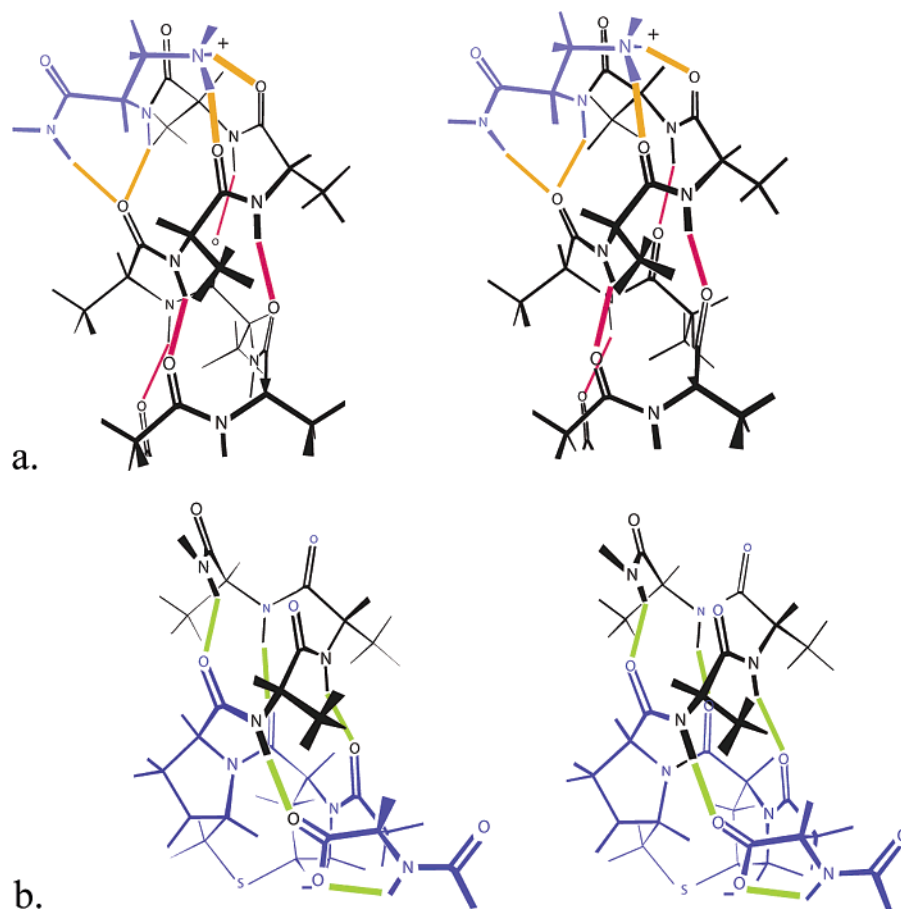


Figure 4. Computer-generated stereodiagrams consistent with ROE data. (a) The Ala₈-beta C-terminus. (b) The β AspHel-Ala₈ N-terminus. Color code: black, Ala₈ bonds and atoms; blue, beta and β AspHel atoms and bonds; red, Ala-Ala H-bonds; orange, Ala₈-beta H-bonds; green, Ala₈- β AspHel H-bonds. Structures were generated by Quanta (Molecular Simulations, Inc.).

TOCSY assignments of CH chemical shifts and connectivities for resonances attributable to the Hel function correspond closely to a previously reported NMR characterization of the Hel function of AcHel-Ala₆-OH.²⁰ The R-CO-Hel function is remarkably rigid, but it embodies three degrees of two-state conformational freedom. Its tertiary N-acylamido group can assume either (c) or (t) orientations; the ψ dihedral angle of its peptide-linked carboxamido function can assume either helical or γ -turn orientations, and its eight-membered lactam can assume either helix-initiating (e) or noninitiating (s) conformations. All are defined for the major NMR conformation. A cross-peak links the resonances assigned to protons at C₁₂ and the β -CH₂ of the Asp function and establishes the orientation of the Asp-Hel amide bond as (t). A cross-peak linking Hel C-9 and C-13 proton resonances establishes the orientation of the eight-membered ring of the Hel function as (e). Three cross-peaks are detected between the resonance of the NH proton of Ala-1 and resonances corresponding to C-6, C-7, and C-8 Hel protons. These establish the orientation of the Hel C-5 ψ dihedral angle as helical.²²

TOCSY, NOESY, and 1D ¹H NMR spectra were also measured at pH 4.5, 2 °C in aqueous buffer for members of the peptide series 2 Ac- β AspHel-beta-AccLys₂TrpNH₂, n even, 8–16. Resonances of the capping regions of these peptides and their NOE cross-peaks with end regions of Ala _{n} were consistent

with those assigned for peptide 1. These assignments correspond to a helix-nucleating (te) state of β AspHel, Figure 4b. Resonances belonging to Ac β Asp exhibit intraresidue cross-peaks, but none defined contacts with the Ala _{n} region. The pH dependences of NH resonances of peptide 1 and selected members of series 2 are more informative. If the pH is varied from 1.5 to 8.5, three correlated changes in chemical shift are observed: 0.45 ppm for the resonance of the NH function of Ac- β Asp, 0.19 ppm for the NH resonance of Ala-1, and 0.13 ppm for the NH resonance of Ala-2. Ionization of the carboxylic acid of Ac- β Asp is expected to have a large chemical shift effect on its own NH, since these groups are proximate. The observed shift changes for Ala₁ and Ala₂ NH resonances imply that in the ionized structure the carboxylate anion is also proximate to these protons.

The titration curve for each chemical shift yields pK_a values of 3.29 in water, 2 to 50 °C, that correspond to ionization of the Asp α -carboxylic acid (Figure 5). This pK_a value, calculated from local chemical shifts of single NH protons, is also assignable from the pH dependence of $[\theta]_{222}$, which reflects the global anion-dipole helix stabilization. Ionization results in a ca. 20% increase in CD fractional helicity for Ala _{n} peptides, $n = 7$ to 9, confirming our postulated role for the carboxylate anion of N-cap β AspHel.⁹

Resonances attributable to a minor conformation can also be detected at low pH in NMR spectra of Ala _{n} peptides. These are assigned, Figure 3, to the previously documented weakly helical

(22) Cammers-Goodwin, A.; Allen, T. J.; Oslick, S. L.; McClure, K. F.; Lee, J. H.; Kemp, D. S. *J. Am. Chem. Soc.* **1996**, *118*, 3082–3090.

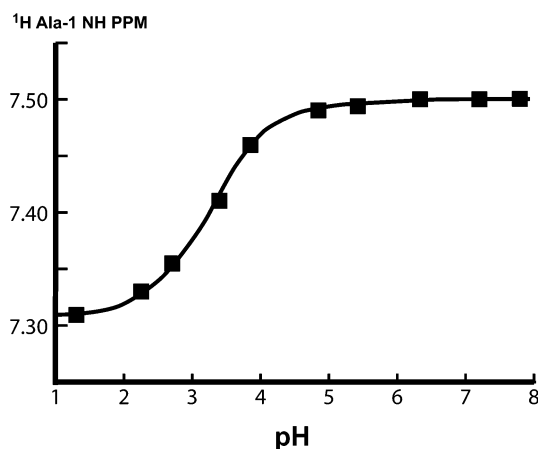


Figure 5. Titration of the β Asp carboxylic acid of Peptide **1** in water at 2 °C, monitored by changes in the chemical shift of the first alanine NH function (similar curves result from monitoring chemical shifts of the second alanine NH or the Asp NH). The curve is calculated from respective limiting chemical shifts for the conjugate acid (7.314 ± 0.003) and base (7.497 ± 0.002) and from an assigned pK_a value at 2 °C of 3.27 ± 0.035 ; at 25 and 49 °C, respective pK_a values of 3.31 ± 0.02 and 3.27 ± 0.02 were assigned.

(cs) state for which the N-cap is a poor helix stabilizer. We have previously introduced t/c , the ratio of integrated areas of (c) and (t) state resonances, as a quantitative measure of helicity and have shown that any experimental variable that increases helical stability also increases t/c .²⁰ Consistent with this assignment, the relative intensity of the resonances of the minor conformations of the peptides **1** and **2** is substantially decreased by helicity-increasing variable changes: lower temperatures, a pH increase above 3.4, an increase in Ala_n length, and addition of trifluoroethanol. The CD and PF_i measurements of this study were conducted in aqueous solutions at 2 °C and above pH 4.5; under these conditions, t/c is large.²³

From the evidence of this section, the C-cap β has been shown to interact locally with the C-terminal loop of the Ala_n sequence, terminating the helical sequence¹⁰ and optimally positioning the positive charge of β for helix stabilization. Above pH 4.5, the ionized N-cap β AspHel assumes the previously characterized (te) conformation that allows two amide oxygens of the Hel function to form donor hydrogen bonds with NHs of the second and third amides of the Ala_n region. The carboxylate anion of the β Asp function is positioned to hydrogen bond with the first amide NH of the Ala_n region, allowing its charge to stabilize the N-terminus of the Ala_n helical conformation initiated by the β AspHel cap. The peptides are unaggregated in water and show no evidence of tertiary structure; NH hydrogen exchange is slow within the Ala_n region but rapid for all other residues; and NMR evidence defines the structures of the β AspHel and β caps and demonstrates their local interactions with the Ala_n region. As summarized in Figure 4a,b, these observations demonstrate peptide-cap interactions of these peptides that are consistent with an Ala_n α -helix and confined to its first three and last three residues.

Assignment of ¹H and ¹³C Chemical Shifts to Alanine Residues of the Ala_n Region

Assignment of protein secondary structures from NMR chemical shifts has received much recent attention. By reference

(23) As detailed in the Experimental Section, for pH values greater than 4.5, and for Ala_n lengths of at least six residues, t/c values ≥ 50 are expected.

to the literature database, protein or peptide chemical shift data can be used to predict local regions of helical structure.²⁴ Helical backbone ¹HN chemical shifts are sensitive to hydrogen bond length and strength, solvent exposure, deviations from helical rod structures, and residue positioning within either the N- or the C-terminus. Experimental constancy of ¹HN shifts thus provides a sensitive test for Ala_n structural convergence.

Resonances of eight Ala ¹HN residues belonging to the two end regions of members of series **2** exhibit distinctive chemical shifts and are consistently resolved. At the N-terminus for the series members with $n = 10$ to 16, chemical shifts for Ala -1 appear in the unusual range 7.48 ± 0.02 ppm, but the ¹HN chemical shifts for Ala -2 and 3 appear within a more normal helical range of 8.37 ± 0.02 ppm. Chemical shifts for Ala -4 fall in the distinctive range 8.11 ± 0.02 ppm, which may reflect a local structural transition from hydrogen bonding acceptor oxygens of tertiary amides of the Hel function to the oxygen of the secondary amide at the Hel- Ala_n junction.

Resonances for ¹HNs at the $(n - 3)$ and $(n - 2)$ sites appear, respectively, at 8.09 ± 0.01 ppm and 8.08 ± 0.01 ppm, and resonances at the $(n - 1)$ and n sites appear, respectively, at 7.93 ± 0.02 and 7.95 ± 0.02 ppm. From the PDB, downfield shifts for ¹HNs at a helical N-terminus and upfield shifts at a C-terminus have been documented and attributed to a helix dipole effect.²⁵ This effect as well as helical fraying at the C-terminus of these peptides may account for these systematic site-specific changes. Corresponding chemical shifts²⁶ for the Ala_8 peptide of series **2** are qualitatively similar. The NMR properties of the eight N-terminal and C-terminal residues of a series **2** Ala_n peptide sequence, $n = 8$ or larger, show characteristic site-dependent values that are independent of the length n .

The ¹HN chemical shifts for resonances found at all remaining sites 5 to $(n - 4)$ within the five peptides of series **2**, $n = 10$ –16 are unresolved, with a mean value of 8.21 ± 0.02 ppm. For the central $n - 8$ residues of these peptides, these ¹H NH chemical shifts demonstrate convergence, consistent with their structural isolation from capping regions.

The chemical shifts of ¹³C=O and ¹³C α functions correlate with FH values²⁷ and are reliable reporters of helical structure within protein sequences.²⁵ Invariably the largest ¹³C chemical shifts are seen for helices. The reported averages for protein-derived values of ¹³C=O chemical shifts of alanine residues within respective β -strand, coil, and helical regions are 175.0, 177.6, and 179.6 ppm; the values of alanine ¹³C α chemical shifts are 50.3, 52.4, and 54.7 ppm. Coil values are in good agreement those observed for short peptides (¹³C=O, 177.6 ppm; ¹³C α , 52.2 ppm), and the helical values are consistent with values assigned from a recent study of a highly helical alanine-rich peptide at 0 °C in water (¹³C=O, 180 ppm; ¹³C α , 54.0 ppm).

To assign ¹³C chemical shifts to members of Ala_n series and to facilitate measurement of other key helicity parameters, three peptides were synthesized containing alanine residues labeled

(24) Wishart, D. S.; Sikes, B. D. *Methods Enzymol.* **1994**, *239*, 363–392.
 (25) Wishart, D. S.; Richards, F. M.; Sikes, B. D. *J. Mol. Biol.* **1991**, *222*, 311–333.
 (26) The following ¹HN chemical shifts (ppm) are seen for the series **2** Ala_n peptide: site 1, 7.50; site 2, 8.29; site 3, 8.26; site 4, 8.00; site 5 ($n - 3$), 8.02; site 6 ($n - 2$), 8.00; sites 7 and 8 ($n - 1$, n), 7.90.
 (27) (a) Shalongo, W.; Dugad, L.; Stellwagen, E. *J. Am. Chem. Soc.* **1994**, *116*, 2500–2507. (b) Werner, J. H.; Dyer, R. B.; Fesinmeyer, R. M.; Andersen, N. H. *J. Phys. Chem. B* **2002**, *106*, 487–494.

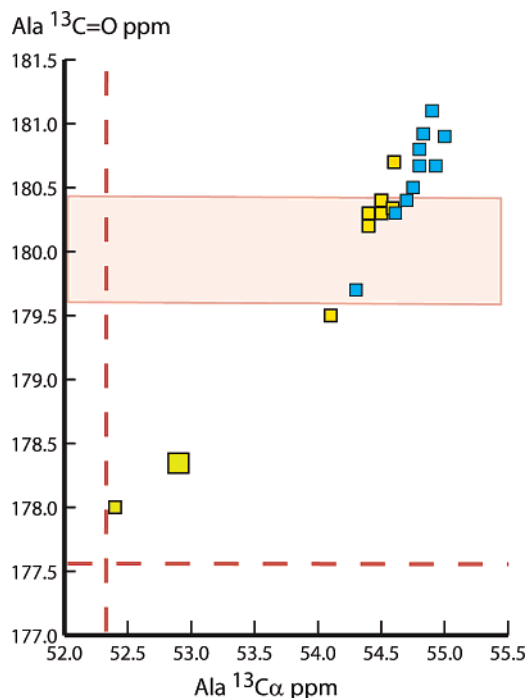


Figure 6. Correlation of $^{13}\text{C}=\text{O}$ and $^{13}\text{C}\alpha$ chemical shifts for the labeled series **2** Ala₈ peptide (water, pH ca. 3) and the Ala₁₂ peptide (water, pH > 4.5). The red dashed lines are derived from the protein database and are an interface between helix and coil values.^{24,25} The pink area defines the average, within one SD unit, of the $^{13}\text{C}=\text{O}$ values reported for a highly helical peptide.²⁷ Pairs of Ala chemical shift values for the Ala₁₂ peptide appear as cyan squares (owing to overlap, only 10 pairs of values are plotted). Pairs for the (te) state of the Ala₈ peptide appear as yellow squares; the small green square corresponds to the chemical shift pair of the Ala-1 (cs) state. The large green square corresponds to the average, within 1 SD, of the remaining (cs) state resonances. (Because of weak signal intensities, residue assignments could not be made.)

with ^{13}C and ^{15}N . Their $^{13}\text{C}=\text{O}$ chemical shifts were assigned from a 2D version, H(N)CO, of a standard HNCOC experiment,²⁸ which correlates a $^{13}\text{C}=\text{O}$ chemical shift for a residue at sequence site i with the previously assigned ^1HN chemical shift at sequence site $i + 1$. An unambiguous assignment requires that no resonance overlaps occur, within either the ^1H or the ^{13}C set. This condition was met by the labeled Ala₈ peptide **1**, but it is unlikely to be met for longer members of series **2**. All Ala resonances of the series **2** Ala₁₂ peptide were assigned ^1H and ^{13}C chemical shifts by studying two peptides, one doubly labeled at alanines 1–6, the other at alanines 7–12.

Figure 6 shows the results of measurement of ^{13}C chemical shifts observed for the $^{13}\text{C}=\text{O}$ and $^{13}\text{C}\alpha$ resonances at 8 °C in aqueous buffer for the labeled peptides. The plot includes red dotted lines that define the literature boundary between helix and coil for alanine residues of the PDB and a pink region that corresponds to the range of $^{13}\text{C}=\text{O}$ chemical shifts reported for the alanine-rich peptide.²⁷ Our Ala₈ peptide was studied at pH 3 at which the helix-stabilizing βAspHel cap functions suboptimally; as a result both its (te) and (cs) state resonances can be detected. With the exception of the borderline resonance that corresponds to the C-terminal alanine, the former lie well within the expected helical regions, and the latter lie close to random coil values.

The Ala₁₂ peptide was studied at pH > 4.5. The majority of its (te) chemical shift pairs fall within the protein helical region,

above the peptide values, with pairs linked with N-terminal Ala residues appearing at the upper right of the Ala₁₂ sequence. The three pairs that lie at or in the pink zone correspond to residues within the Ala₁₂ C-terminal loop. Like the site dependence of ^1H NH chemical shift values, this pattern is consistent with progressive helical fraying toward the Ala₁₂ C-terminus. For the core Ala-5 and Ala-6 residues of this sequence, the carbonyl carbon shifts are identical, 180.90 ppm, as are α -carbon chemical shifts, 54.87 ppm; these lie at the upper end of values assigned from protein structures. These are the convergent values for ^{13}C chemical shifts of alanine residues within core helical regions of polyalanines in water at 2 °C.

Chemical shift data can be diagnostic for helical structure, but detailed conformational assignments are usually based on NOEs, which for Ala_{*n*} peptides require site-labeled peptides.²⁹ Even with a definitive labeled series, 3_{10} - α structural distinctions can be problematic. As noted recently,³⁰ a more reliable alternative is available. The modified H(N)CO NMR experiment of Cordier and Grzesiek^{31,32} yields ^{15}N – $^{13}\text{C}=\text{O}$ scalar couplings $^3J_{\text{NC}'}$ that directly define helical amide–amide ^{15}N – $\text{H}\cdots\text{O}=\text{C}$ hydrogen bonds.

The schematic of Figure 1a identifies pairs of alanine residues of a labeled Ala₈ peptide with ^1H and ^{13}C nuclei that are expected to exhibit scalar α -helical $^3J_{\text{NC}'}$ couplings. For a peptide with n labeled alanines, the modified H(N)CO NMR experiment should exhibit $n - 4$ cross-peaks that correspond to hydrogen bonds that link $^{13}\text{C}=\text{O}$ at each site i with a ^1H – ^{15}N at site $(i + 4)$. For the series **1** Ala₈ peptide in which all Ala residues are uniformly labeled with ^{13}C and ^{15}N , the following four residue pairs should show a $^3J_{\text{NC}'}$: 1 and 5, 2 and 6, 3 and 7, 4 and 8.³³ Figure 7a shows results of applying the 2D H(N)CO experiment to this peptide. (It should be noted that the seven purple $i, i + 1$ cross-peaks allow assignment of covalent amide connectivities and the $^{13}\text{C}=\text{O}$ chemical shifts of Figure 6.) The four green α -helical $i, i + 4$ cross-peaks correspond to $^3J_{\text{NC}'}$ scalar couplings that link residues 1 with 5 and 2 with 6; a confluent region defines the couplings that link residues 3 with 7 and 4 with 8. These verify the α -helical structure.

Figure 7b shows the corresponding 2D spectrum for the series **2** Ala₁₂ peptide in which residues 7–12 were labeled. An α -helical hydrogen bonding pattern requires that the spectrum should reveal two α -helical $^3J_{\text{NC}'}$ scalar couplings that link residues 7 with 11 and 8 with 12. Both of these are evident. Application of the same experiments to the Ala₁₂ peptide with labeled sites Ala-1 through Ala-6 confirmed the presence of α -helical hydrogen bonds that link amides of residue 1 with 5 and 2 with 6 (spectrum not shown).

For the labeled Ala₁₂ peptide of Figure 7b, the presence of significant contributions of conformations with 3_{10} helical structure should be signaled by appearance of cross-peaks corresponding to hydrogen bonds that link residues 7 with 10,

(29) Kemp, D. S.; Allen, T. J.; Oslick, S. L.; Boyd, J. G. *J. Am. Chem. Soc.* **1996**, *118*, 4240–4248.

(30) Dehner, A.; Planker, E.; Gemmecker, G.; Broxterman, Q. B.; Bisson, W.; Formaggio, F.; Crisma, M.; Toniolo, C.; Kessler, H. *J. Am. Chem. Soc.* **2001**, *123*, 6678–6686.

(31) Dingley, A.; Grzesiek, S. *J. Am. Chem. Soc.* **1998**, *120*, 8293–9297.

(32) Cordier, F.; Grzesiek, S. *J. Am. Chem. Soc.* **1999**, *121*, 1601–1602.

(33) For the N- and C-capped Ala_{*n*} peptides of this study, one could in principle demonstrate four more hydrogen bonds between the caps and the Ala_{*n*} region if the appropriate $^{13}\text{C}=\text{O}$ labeled βAspHel and of ^{15}N labeled β were available.

(28) Grzesiek, S.; Bax, A. *J. Magn. Reson. Ser.* **1992**, *96*, 432–440.

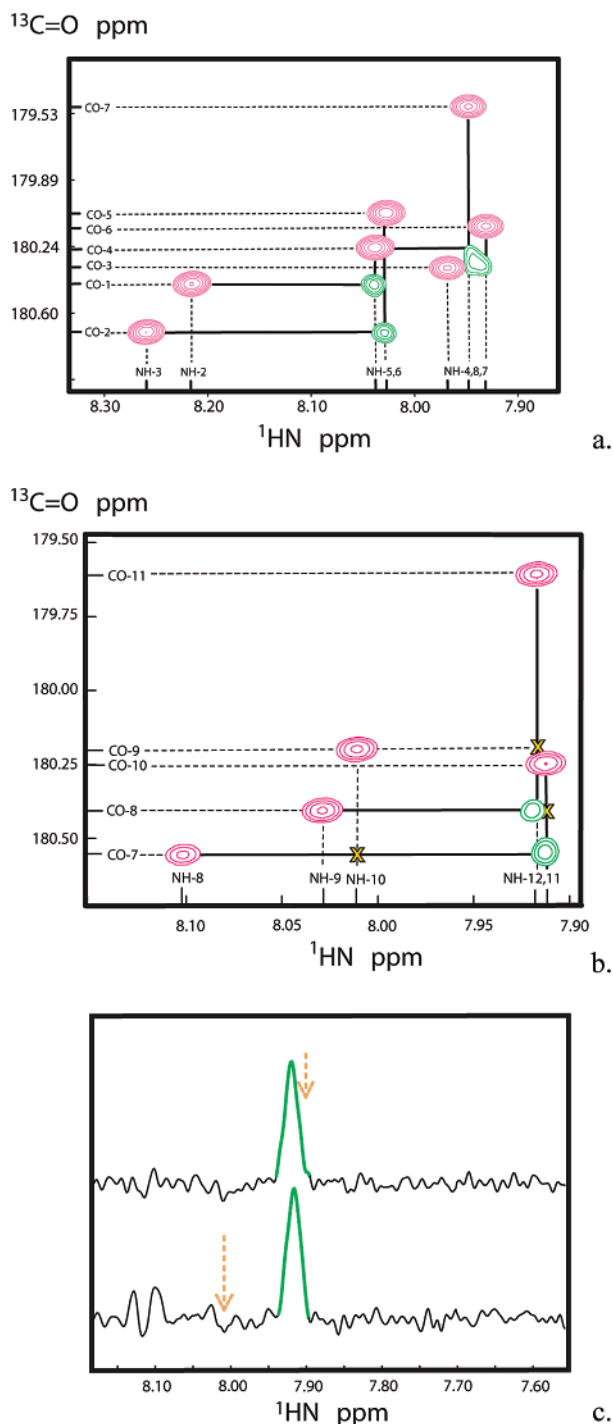


Figure 7. Assignment of dominant α -helical structure to the ^{13}C - and ^{15}N -labeled peptides Ala₈, **1**, and Ala₁₂, **2**. (a) Results of 2D H(N)CO NMR experiments in water at 10 °C, pH > 4.5, applied to Ala₈. Cross-peaks (magenta) result from an experiment with dephasing time optimized for correlation of chemical shifts for a site i $^{13}\text{C}=\text{O}$ with the site $i + 1$ ^1HN . Cross-peaks (green) result from a dephasing time optimized for detection of $^3J_{\text{NC}}$ scalar coupling. These demonstrate hydrogen bonds linking residues 1 and 5, 2 and 6, and through a confluent pair of cross-peaks, 3 and 7, 4 and 8: an α -helix. (b) Results of application of the experiments of Figure 7a to the Ala₁₂ peptide with six labeled C-terminal residues. The green cross-peaks correspond to the expected α -helical hydrogen bonds that link residues 7 with 11 and 8 with 12. Gold crosses mark the expected positions for $^3J_{10}$ $^3J_{\text{NC}}$ coupling; these cross-peaks are not detected. (c) Top spectrum: a slice of an optimized Figure 7b spectrum at the residue 8 $^{13}\text{C}=\text{O}$ resonance (180.45 ppm). Bottom spectrum: a corresponding slice for residue 7 (180.61 ppm). Gold arrows identify sites of undetected $^3J_{10}$ cross-peaks.

8 with 11, and 9 with 12. In the figure, the sites of these potential cross-peaks are indicated by gold crosses. Even for the 7, 10 link, which would appear without overlap, no cross-peak is evident. This issue is explored more rigorously in Figure 7c, which shows optimized 1D slices measured at the $^{13}\text{C}=\text{O}$ chemical shifts of the Figure 7b green cross-peaks. No $^3J_{10}$ cross-peak can be detected within the signal-to-noise limits of the experiment.

If an amino acid sequence has been independently established as α -helical, the $^3J_{\text{HNH}\alpha}$ coupling constant defines the ϕ dihedral angle, which for an α -helix can fall in the range of -30 to -80° . An α -helix has a parametric dihedral constraint, $\phi + \psi = -103^\circ$, allowing ψ to be defined from the assigned ϕ .³⁴ The ϕ value for the Pauling–Corey helix³⁵ is -47° , and that assigned by Arnott and Dover² from an X-ray fiber diffraction study of polyalanine is -57.4° , but the average value for helices within the PDB is $-62 \pm 7^\circ$.³⁶

The $^3J_{\text{HNH}\alpha}$ coupling constants were assigned to the helical alanine residues in the three peptides from an E.COSY HNCA experiment.³⁷ The average for the twelve amino acids of the series **2** Ala₁₂ peptide in water at 2 °C is 3.4 Hz (SD 0.5), and the pair of core alanines at sites 5 and 6 showed identical values of 3.0 Hz. Fits of the latter value to the Karplus equation using parameters of Vuister,³⁸ Pardi,³⁹ and Ludvigsen⁴⁰ yield respective ϕ values of -50.4° , -48.6° , and -52.7° . The average of these is close to that of the Pauling–Corey and the Arnott–Dover ϕ values but substantially lower than the average assigned by Barlow and Thornton from the X-ray crystallographic protein database.

Protection Factors PF_{*i*} for Ala ¹HN functions of the Peptide Series 2 and 3

Protection factors PF_{*i*}'s measured for the series **2** Ala_{*n*} peptides allow a residue-by-residue assignment of helicity, and this quantitative energetic characterization complements the NMR structural assignments. PF_{*i*}'s provide the definitive test of the efficiency of helix stabilization by the β AspHel N-cap and *beta* C-cap, and for representative members of series **2** and **3** they allow calculation of length-dependent FH values. For series **2**, they also allow calculation of site helicities FH_{*i*}.

A PF_{*i*} defines the relative tendency of a backbone amide NH_{*i*} at site i of a peptide or protein sequence to undergo an NH_{*i*} → ND_{*i*} exchange reaction in D₂O. An amide NH_{*i*} that is part of the H-bonded structure of completely helical peptide exchanges very slowly.⁴¹ The exchange rate for an NH at site i of a frayed helix reflects the presence of conformers in which the amide NH_{*i*} is nonhelical and solvent exposed. A PF_{*i*} is defined, eq 2,

$$\text{PF}_i = k_{2\text{NHSid}}/k_{2\text{PeptideNH}_i} \quad (2)$$

as the ratio of two rate constants, $k_{2\text{PeptideNH}_i}$, the exchange rate constant for an NH at site i of a partially helical peptide, and

- (34) Besley, N. A.; Hirst, J. D. *J. Am. Chem. Soc.* **1999**, *121*, 9636–9644.
 (35) Pauling, L.; Corey, R. B.; Branson, H. R. *Proc. Natl. Acad. Sci. U.S.A.* **1951**, *37*, 205–211.
 (36) Barlow, D. J.; Thornton, J. M. *J. Mol. Biol.* **1988**, *201*, 601–619.
 (37) Weisemann, R.; Rüterjans, H.; Schwalbe, H.; Schleucher, J.; Bermel, W.; Griesinger, C. *J. Biomol. NMR* **1994**, *4*, 231–240.
 (38) Vuister, G. W.; Bax, A. *J. Am. Chem. Soc.* **1993**, *115*, 7772–7777.
 (39) Pardi, A.; Biller, M.; Wüthrich, K. *J. Mol. Biol.* **1984**, *180*, 741–751.
 (40) Ludvigsen, S.; Andersen, K. V.; Poulsen, F. M. *J. Mol. Biol.* **1991**, *217*, 731–736.
 (41) Englander, S. W.; Kallenbach, N. R. *Q. Rev. Biophys.* **1983**, *16*, 521–655.

$k_{2\text{NHStd}}$, the exchange rate constant for solvent-exposed NH in a simple, analogous model peptide. The atom fraction of the solvent-exposed NH proton is calculated as $1/\text{PF}_i$, and eq 3

$$\text{FH}_{\text{NH}_i} = 1 - 1/\text{PF}_i \quad (3)$$

defines the fraction of the NH_{*i*} that is hydrogen bonded within a helical structure, which is FH_{NH_i} , a measure of local helicity.

Although the ¹³C=O and ¹³Cα chemical shifts of an *i*th amino acid residue can also be used to calculate site helicity FH_i ,²⁷ FH_{NH_i} is more valuable for study of highly helical peptides. The chemical shift reflects the fraction of the conformer population that is helical at a ¹³C site, but a PF_i is proportional to the fraction of nonhelical conformers, which varies by a factor of 10 if FH_i increases from 0.90 to 0.99. PF_i 's can be used to draw fine distinctions within a series of highly helical sites.⁴²

Practical features of the measurement of PF_i 's have been reported by Englander et al.; these include quantitative effects of pertinent experimental variables and a database of reference rate constants $k_{2\text{NHStd}}$ needed to calculate PF_i 's.¹¹ At a given pH the overall exchange rate constant is a sum of acid- and base-catalyzed terms, but for normal peptides studied at pH values greater than 3.5, the base-catalyzed mechanism dominates and the second-order rate constant depends on concentrations of hydroxide and substrate as well as temperature and the hydrophobic bulk and charge of the two amino acids that flank the exchanging amide NH_{*i*}. Corrections for these effects have been reported.¹¹

The PF_i measurements for Ala NH_{*i*}'s of series 2 and 3 peptides were carried out in D₂O at 2 °C. Rates were measured at pH values above 4.5 and were followed for at least three half-lives by analyzing both peak heights and curve-fitted areas for the ¹HN NMR resonances. Rate constants for series 2 and 3 peptides were in reasonable agreement.

As noted earlier, the presence of multiple Inp residues within the sequences of series 3 peptides results in substantial broadening and overlap of the ¹HN resonances. The normal resonance widths observed for series 2 peptides allowed PF_i and FH_{NH_i} site assignments to the four NHs at the N-terminus of each Ala_{*n*} sequence and to the corresponding four NHs at the C-terminus. Figure 8 plots averages with standard deviations of these PF_i 's at each Ala NH site. The central region of the graph plots averages of PF_i 's for the 20 nearly coincident resonances of the Ala_{*n*} cores of series 2 peptides. These averages exceed 100, and with their likely error limits, they define limiting core FH_{NH_i} values as lying within the range 0.990 to 0.994. Individual resonances usually could not be resolved for series 3 peptides, but the time dependences of the collective integrated ¹HN resonance intensities were compared for the two series and were found to agree within measurement error.

What structural properties of a peptide helix are reflected by an FH_{NH_i} value? Each FH_{NH_i} corresponds to the overall mole fraction of peptide conformers for which the amide NH at site *i* forms a helical H-bond. This bond can be formed, only if each of the sets of ϕ and ψ dihedral angles at α -carbons allow the three preceding residues to form helical H-bonds. An FH_{NH_i}

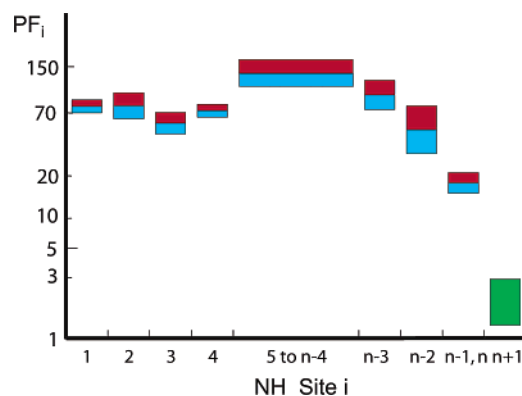


Figure 8. Average values of protection factors PF_i 's measured in D₂O at 2 °C pH > 4.5 for Ala_{*n*} regions of series 2 peptides with *n* > 8. Variations within one SD unit are shown as red and blue bars; the green region corresponds to the low average and large range of uncertainty for PF_{n+1} (see text for details).

thus corresponds to the relative abundance of conformations that are helical at sites (*i* - 1), (*i* - 2), and (*i* - 3).

Figure 1c depicts the sequence of hydrogen bonds that can be formed by the amide residues of a representative Ala_{*n*} region of series 2 and 3 peptides. Three of these are absent for an Ala_{*n*} region that is N-capped by an acetyl and C-capped by an NH₂. The green hydrogen bonds are common to both regions and consists of bonds formed between pairs of Ala amides or that are formed between a single Ala amide NH at site 4 and *N*-acyl carbonyl oxygen or the (*n* - 3) amide carbonyl and the C-terminal NH. The first three NH sites of a simple Ac-Ala_{*n*}-NH₂ are solvent exposed, their PF_i values at these sites equal 1.0, and their corresponding FH_{NH_i} equal 0. As assigned from experimental PF_i , helical stability for a peptide of length *n* is defined by (*n* - 2) nonzero FH_{NH_i} 's at sites *i* = 4 through (*n* + 1).

We have proposed the blue hydrogen bonds of Figure 1c as linking NH residues of the first three residues of the helix to oxygens of the β AspHel N-cap. The PF_1 , PF_2 , and PF_3 values reported in Figure 8 demonstrate their presence and their helix-initiating efficiency. These PF_i correspond to FH_{NH_i} values of 0.98 to 0.99. The value of FH_{NH_1} solely reflects interactions of the first peptide NH with the N-cap. Formation of an intramolecular hydrogen bond by the NH of Ala-1 requires adoption of the helix-initiating (te) conformation by β AspHel, and the magnitude of FH_{NH_1} corresponds to a *t/c* value equal to or greater than 50, in accord with the estimates cited in earlier sections. The values for FH_{NH_2} and FH_{NH_3} reflect the adoption of helical ϕ , ψ angles by residues 1 and 2, a structural precondition for formation of hydrogen bonds between their NHs and carbonyl oxygens of the pair of tertiary amides within the Hel function. Finally, FH_{NH_4} reflects the energetics of formation of the α -helical loop that defines helical ϕ , ψ angles for the first three residues of the Ala_{*n*} sequence. The small standard deviations and similar values seen for FH_{NH_1} , FH_{NH_2} , FH_{NH_3} , and FH_{NH_4} suggest that no structural mismatch occurs at the junction between the N-terminus of the peptide helix and the preorganized β AspHel N-cap. They confirm the presence of the H-bonds of Figures 1c and 4b. A total of (*n* + 1) nonzero FH_{NH_i} 's characterize sites *i* = 1 through (*n* + 1) of series 2 and 3 peptides.

The remaining (*n* - 2) PF_i 's of Figure 8 characterize the helicity of the Ala_{*n*} region itself, and those defined at sites 4

(42) This point is demonstrated by trios of values for (1) PF_i in the range of 2 to 100, (2) FH_{NH_i} calculated from eq 4, and (3) the percent error in FH_{NH_i} under the assumption of a 10% error in PF_i . For example: 2, 0.5, 24%; 5, 0.80, 7%; 10, 0.90, 2%; 20, 0.95, 1%; 50, 0.98, 0.4%; 100, 0.99, 0.2%. PF_i values of 50 ± 5 thus allow assignment of FH_{NH_i} with greater than two-decimal-place precision.

through n reflect NH \rightarrow ND exchange properties of Ala NH residues. An additional PF_i at site $(n + 1)$ reflects the relative exchange rate of the α -amide NH of the C-capping function *beta*. It monitors local helicity for the three contiguous residues at the Ala $_n$ C-terminus. Owing to the rapid exchange of this NH at a pH $>$ 4.5, accurate time-dependent rates could not be assigned, but upper and lower bounds for $PF_{(n+1)}$ were estimated from the pH dependence of the NH resonance broadening in H₂O within a pH region where intermediate line broadening due to proton exchange is observed. Calibration through measurement of an exchange rate for an Ala NH in a short model peptide showed consistency with PF_i values measured at internal Ala $_n$ sites. The resulting helicity limits are $0.1 < FH_{NH(n+1)} < 0.7$.

A monotonic decrease with length is seen for PF_{n-3} , PF_{n-2} , PF_{n-1} , and PF_n values. A plot of PF_i vs site for a helical peptide that lacks strong cap stabilization has an inverse parabolic appearance with a maximal value at site $i = (n/2 + 2)$ and values at the terminal sites 4 and $(n + 1)$ that can fall below 1.1.^{8,11} The C-terminal length decrease seen in Figure 8 is much less dramatic. The PF_n for the C-terminal Ala NH is slightly below 20, corresponding to an FH_{NHn} of 0.94. This value is consistent with substantial helical stabilization by the positively charged C-terminal *beta*, consistent with the positioning of its ammonium ion at the C-terminus, as seen in Figure 4a.

What is the relationship between the set of FH_{NH_i} assigned for the series 2 peptides and the corresponding site helicities FH_i ? An FH_i is defined as the atom fraction of helical α -carbons at site i , and an Ala $_n$ peptide has one FH_i for each Ala α -carbon. Their average is the peptide fractional helicity, FH. Each of the $(n - 2)$ FH_{NH_i} reflects local three-residue helicity at sites $(i - 1)$, $(i - 2)$, and $(i - 3)$, and as seen in eq 4,

$$FH_{NH_i} \leq (FH_{i-3} + FH_{i-2} + FH_{i-1})/3 \quad (4)$$

the value of FH_{NH_i} sets a lower bound for the average of the values of FH_{i-1} , FH_{i-2} , and FH_{i-3} .⁴³ If the value of a PF_i approaches or exceeds 100, the lower bound can be replaced to a good approximation by an equality. For example, if FH_{NH4} closely approaches 1.0, so must FH_1 , FH_2 , and FH_3 . If, in addition, the contiguous $FH_{NH5} \approx 1.0$, then $FH_4 \approx 1.0$. This pair of FH_{NH_i} defines the values of four FH_i 's. Generalizing this result to a region, one sees that if the values for FH_{NH_i} for j contiguous NHs are close approximations to 1.0, it follows that $j + 2$ of the associated FH_i are also approximated by 1.0. The sets of n FH_i and $(n - 2)$ FH_{NH_i} thus contain equivalent conformational information. As shown in the Supporting Information, the inequalities of eqs 5 and 6

$$\text{For } FH_{NH_i} > 0.9, \text{ and } i < n/2, FH_{i-3} \approx FH_{NH_i} \quad (5)$$

$$\text{For } FH_{NH_i} > 0.9, \text{ and } i > n/2, FH_{i-1} \approx FH_{NH_i} \quad (6)$$

allow assignment of FH_i values for sites at or near the ends of an Ala $_n$ sequence. The case of an Ala₁₂ peptide is representative. At sites 5 through 8, the FH_{NH_i} values are 0.992, implying that $FH_i \geq 0.99$ at sites 2 through 7. At site 4, FH_{NH_i} assumes a

(43) As detailed previously⁸ (also see Supporting Information) the conformations of the manifold for FH_{NH_i} consist of the logical intersection of sets of conformations that define the values of FH_{i-1} , FH_{i-2} , and FH_{i-3} . For highly helical peptides and for either small or large values of i , this intersection set is closely approximated by the conformations of the manifold associated with the smallest FH_i .

Table 1. Length-Dependent FH Values for Series 2 Ala $_n$ Peptides in Water at 2 °C

n	calculated FH ^a	extrapolated FH ^b	extrapolated $\langle n \rangle$ ^c
8	0.862, 0.944	0.90 \pm 0.04	7.2 \pm 0.3
9		0.91 \pm 0.04	8.2 \pm 0.4
10	0.888, 0.954	0.92 \pm 0.03	9.2 \pm 0.3
11		0.92 \pm 0.03	10.1 \pm 0.3
12	0.905, 0.961	0.93 \pm 0.03	11.2 \pm 0.4
14	0.918, 0.966	0.94 \pm 0.03	13.2 \pm 0.4
16	0.927, 0.970	0.95 \pm 0.02	15.2 \pm 0.3
18		0.95 \pm 0.02	17.1 \pm 0.4
20		0.96 \pm 0.02	19.2 \pm 0.4
22		0.96 \pm 0.02	21.1 \pm 0.4
24		0.96 \pm 0.02	23.0 \pm 0.5

^a The two series of FH correspond respectively to $FH_n = 0.1$, combined the lower limits for other FH_i 's for the series 2 peptides, and to $FH_n = 0.7$, combined with the upper limits for other FH_i 's. ^b Values calculated from values in the first two columns, as described in the text and Appendix section of the Supporting Information. ^c $\langle n \rangle = nFH$.

slightly lower value, 0.987, which, from eq 5, can be assigned to FH_1 . Application of eq 6 yields all but one of the remaining assignments: $FH_{NH9} = FH_8 = 0.988$; $FH_{NH10} = FH_9 = 0.986$; $FH_{NH11} = FH_{10} = FH_{NH12} = FH_{11} = 0.955$. Generalized to the series 2 Ala $_n$ peptides for $n > 8$, this analysis yields FH_i assignments for Ala sites of series 2 peptides. Setting $FH_{12} = FH_{NH13}$ yields the previously defined lower and upper limits of 0.1 and 0.7.

For a series 2 Ala $_n$ peptide and a given value of n , the average of all FH_i values is its overall fractional helicity FH, and the sum of all FH_i values is the average helical length $\langle n \rangle$, eq 7.

$$(1/n)\Sigma FH_i \equiv FH; n FH = \Sigma FH_i = \langle n \rangle \quad (7)$$

By averaging the lower and upper bounds of error limits for each FH_i value, lower and upper bounds for FH were calculated, and these are listed in the first and second columns of Table 1. Consistent with this analysis, interpolated and extrapolated length-dependent values are calculated by deleting or adding core values to the calculation, as described in the Supporting Information. The averages and ranges of these are given in the third column. Multiplication of each value by n yields values and ranges for the average helical lengths $\langle n \rangle$; clearly $\langle n \rangle \approx n - 1$.

The CD analysis of the following section relies on series 3 data, and an essential issue is a confirmation that the FH values of Table 1, which were derived from series 2 data, are relevant to the CD analysis. This confirmation can be obtained by applying the same FH criterion to members of both data sets. Weighted averages of PF values derived from time-dependent integrations of the entire Ala $_n$ NH resonance region for series 2 peptides, $n = 14$ and 16, yield a mean FH of 0.94 ± 0.02 . Similar averages of PF values were conducted for series 3 peptides and converted to FH values to yield, for $n = 18$, 0.95 ± 0.02 , and, for $n = 22$, 0.955 ± 0.02 . These are within the error limits of the corresponding values seen in the third column of the table. This finding justifies application of its extrapolated FH and $\langle n \rangle$ value to CD data for both peptide 2 and peptide 3 series.

The results of all NMR analyses can be summarized. (1) The helical region is confined to the Ala $_n$ sequences, which form α -helices with ϕ angles consistent with polyalanine fiber diffraction data. (2) From NOEs and modeling evidence, ¹H–¹H contacts detected between the N-cap and the C-cap Ala $_n$

sequence occur, respectively, with the first and last three sequence residues, as depicted in Figures 1c and 4. (3) For $n > 8$, both chemical shifts and PF measurements identify core regions of length $n - 8$, consisting of Ala residues with essentially invariant NMR properties. (4) For the pairs of four residues at the cap-Ala_{*n*} junctions, both chemical shifts and PF_{*i*} values depend on the site *i* but are independent of the overall *n*. (5) The FH_{*i*} values for residues in the core regions exceeds 0.99. (6) The mean Ala_{*n*} FH at 2 °C in water lies in the range 0.90 to 0.96.

These data are consistent with the principle advanced in an earlier section, that the structural effects of the helix-stabilizing N- and C-caps of the Ala_{*n*} peptides of series 2 and 3 should perturb helix structure locally, but not globally. Deviations from core helical properties are confined to the eight Ala residues at the helix ends. This is the necessary condition for applying 2 and 3 Ala_{*n*} peptides $n > 8$ as standards for CD calibration.

Assignment of Core Per Residue Molar Ellipticities [θ] _{λ,∞} from Experimental Molar Ellipticities [θ]_{Molar, λ,n} for Series 3, $n = 9$ through 24, and Series 2, $n = 10$ through 16; Calculation of the Limiting Polyalanine CD Spectrum in Water at 2 °C. Calculation of the Limiting Polyalanine CD Spectrum in Water at 2 °C. Assignment of the Length Parameter X

The use of eq 8 and eq 1 to calculate FH values for peptides and local sequences of proteins from experimental CD residue ellipticities [θ]_{222,*n*,Exp} has a long history.¹⁶ Owing to the strength of the limiting helical ellipticity [θ]_{222,*n*} relative to that of other conformations, the rigorous form of eq 8 is commonly approximated as a simple ratio of experimental to limiting residue ellipticities.

$$FH = ([\theta]_{222,n,Exp} - [\theta]_{222,RC}) / ([\theta]_{222,n} - [\theta]_{222,RC}) \doteq [\theta]_{222,n,Exp} / [\theta]_{222,n} \quad (8)$$

$$[\theta]_{222,n} = [\theta]_{222,\infty} (1 - X/n) \quad (1)$$

Recent developments have increased the accuracy with which protein conformations can be assigned from CD data for proteins of known native structure, and more than thirty years of deconvolution of CD spectra for highly helical proteins of known native structure^{44,45} have provided reasonably satisfactory assignments for the empirically defined parameters *X* and [θ] _{λ,∞} of eq 1. However, errors of fit to helices of the protein database remain large.³⁴ Extrapolations of solvent dependencies for the CD properties of helical alanine-rich peptides of short-to-medium length have also yielded values for *X* and [θ] _{λ,∞} that are in approximate agreement with protein assignments,⁴⁶ although the assumptions underlying these extrapolations have been recently questioned.¹² FH values calculated in this manner are used to rank the “ballpark” helicities of heteropeptides and to monitor temperature or denaturant-induced unfolding of helical proteins.⁴⁷

A more recent role for CD-derived FH values requires a higher accuracy. Predictive algorithms, constructed to assign peptide helicity from amino acid structure and sequence, are often based on FH values calculated from [θ]_{222, Exp} data measured for host–guest substitutions in alanine-rich peptides.^{13a,b} We have recently argued that spaced, solubilized Ala_{*n*} peptides, Figure 1a, are the natural hosts for host–guest helicity studies,⁵ and as a preliminary to host–guest studies, we have presented CD and *t/c* evidence characterizing helical propensities for the Ala residue.^{5b,c} We have also noted that literature values for [θ] _{λ,∞} fail as satisfactory models for the CD properties of (Ala₄Lys)_{*n*} peptides and polyalanines, which usually exhibit exceptionally large ratios of [θ]₂₂₂ to [θ]₂₀₈ as well as curved parametric plots of temperature-dependent [θ]₂₂₂ vs [θ]₂₀₈ data.^{12b} Using the calibration peptides of this study, we now clarify these issues.

$$[\theta]_{\text{Molar},\lambda,\text{Ala},n} = n[\theta]_{\lambda,n} = n[\theta]_{\lambda,\infty} - X[\theta]_{\lambda,\infty} \quad (9)$$

$$[\theta]_{\text{Molar},\lambda,\text{Ala},n} = [\theta]_{\lambda,\infty}(n - k) + [\theta]_{\lambda,\infty}(k - X) \quad (9')$$

$$[\theta]_{\text{Molar},\lambda,n,\text{Exp}} = [\theta]_{\text{Molar},\lambda,\text{AlaCore},n} + [\theta]_{\text{Molar},\lambda,\text{SS-Caps}} = [\theta]_{\lambda,\infty}(n - k) + [\theta]_{\text{Molar},\lambda,\text{SS-Caps}} \quad (10)$$

As a preliminary to data analysis, we rewrite eq 1 as its molar equivalent, eq 9. With no loss of generality, eq 9 can be rewritten as 9', which introduces a parameter *k* that corresponds to the number of alanine residues of Ala_{*n*} with ellipticity contributions that are perturbed from core values by capping or other end effects. The NMR data of preceding sections suggest an assignment of *k* = 8, subject to CD validation.

Two assumptions underlie application of eqs 1 and 9' and their equivalent, eq 10, to the calibration series.⁴⁸ First, for any series 2 or 3 peptide that contains an Ala_{*n*} core with convergent properties, the value of [θ]_{Molar, λ,n ,Exp} can be accurately approximated as a sum of two regional molar ellipticities, [θ]_{Molar, λ,core} and [θ]_{Molar, $\lambda,\text{SS-Caps}$} ; second, the former, which is the core molar ellipticity, can be written as [θ] _{λ,∞} (*n* - *k*), where (*n* - *k*) is the core length, and [θ] _{λ,∞} is the constant incremental increase in peptide molar ellipticity that results if a core region length is increased by one residue.

Figure 9 shows λ -plots of [θ]_{Molar, λ,n ,Exp} for five representative lengths of the series 3 peptides for which $n > 8$. The evident strong length dependence reflects dominance of ellipticities attributable to the Ala_{*n*} cores over the capping effects, which include ellipticity contributions by the first and last four residues of the Ala_{*n*} sequence. In the previous section, PF_{*i*} measurements for core regions were observed to be length independent, with limiting FH_{*i*} values of at least 0.99. This result implies that the per residue increase in [θ]_{Molar, λ,n ,Exp} does not reflect a length-dependent increase in FH_{*i*}. It must be attributed to the incremental effect of adding a new, fully helical Ala residue.

Is [θ]_{Molar, $\lambda,\text{SS-Caps}$} in fact length-independent, consistent with the length independence of ¹H chemical shifts and PF_{*i*}'s (Figure 8), and as required by eq 10? A first answer is provided by calculated regression intercepts for $n = 8$, which can be

(44) (a) Greenfield, N. J. *Anal. Biochem.* **1996**, *235*, 1–10. (b) Sreerama, N.; Venyaminov, S. Y.; Woody, R. W. *Anal. Biochem.* **2000**, *287*, 243–251. (45) (a) Woody, R. W. *J. Polym. Sci. Macromol. Rev.* **1977**, *12*, 181–320. (b) Manning, M. C.; Woody, R. W. *Biopolymers* **1991**, *31*, 569–586. (46) (a) Gans, P. J.; Lyu, P. C.; Manning, M. C.; Woody, R. W.; Kallenbach, N. R. *Biopolymers* **1991**, *31*, 1605–1614. (b) Scholtz, J. M.; Qian, H.; York, E. S.; Stewart, J. M.; Baldwin, R. L. *Biopolymers* **1991**, *31*, 1463–1470. (c) Luo, P.; Baldwin, R. L. *Biochemistry* **1997**, *36*, 8413–8421. (47) Peterson, R. W.; Nicholson, E. M.; Thapar, R.; Klevit, R. E.; Scholtz, J. M. *J. Mol. Biol.* **1999**, *286*, 1609–1619.

(48) For a detailed discussion of this point, see the Supporting Information. The equivalence of eqs 1, 9', and 10 follows directly from: $X \equiv k - [\theta]_{\text{Molar},\lambda,\text{SS-Caps}} / [\theta]_{\lambda,\infty}$; the ratio of this assignment scales the molar ellipticity [θ]_{Molar, $\lambda,\text{SS-Caps}$} as a length by dividing it by the core per residue molar ellipticity, [θ] _{λ,∞} ; *X* is thus the difference between the actual length *k* and this scaled length.

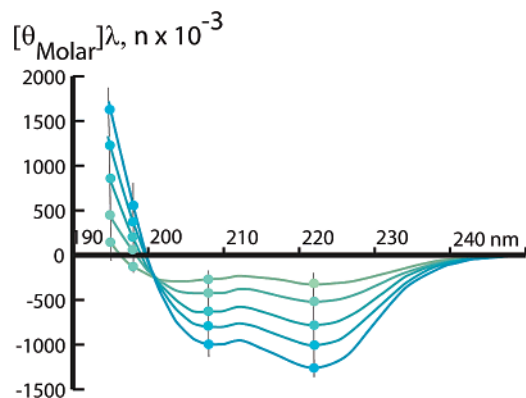


Figure 9. Wavelength plots of $[\theta]_{\text{Molar}}]_{\lambda,n,\text{Exp}}$ for series 3 Ala_n peptides in water pH > 4.5, 2 °C. Units: $\text{deg cm}^2 \text{dmol}^{-1}$. Spectra increase in intensity through the series $n = 9$ (green), 12, 16, 20, 24 (blue-green).

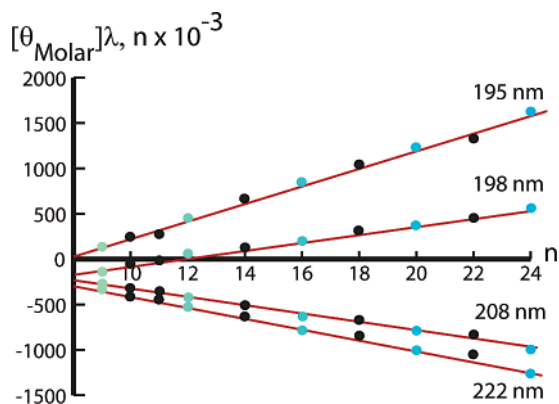


Figure 10. Length-dependent linear regressions at four wavelengths of $[\theta]_{\text{Molar}}]_{\lambda,n}$ for series 3 Ala_n peptides, $n > 8$. Units: $\text{deg cm}^2 \text{dmol}^{-1}$. Data from the spectra of Figure 9 appear as correspondingly colored dots. Extrapolated values for $k = 8$ appear at the intersection of the red lines with the vertical axis.

compared with the experimental values for $[\theta]_{\text{Molar}}]_{\lambda,8,\text{Exp}}$. At all wavelengths, these values agree within measurement errors. Data at 201 nm provide a second answer. At this wavelength, the contribution to $[\theta]_{\text{Molar}}]_{\lambda,n,\text{Exp}}$ from the Ala_n helix vanishes, consistent with the isoellipsoidal point of Figure 9. Equation 10 is reduced to its second term. The values of $[\theta]_{\text{Molar}}]_{201,n,\text{Exp}}$ in units of $10^3 \text{deg cm}^2 \text{dmol}^{-1}$ for the 10 series members are $n = 9, -254.3; 10, -255.6; 11, -250.6; 12, -254.6; 14, -253.6; 16, -265.2; 18, -242.5; 20, -245.0; 22, -233.0; 24, -277.2$. The ellipticity-length correlation coefficient is -0.002 . There is no detectable length dependence of the capping contribution.

At constant λ , from eq 10, $[\theta]_{\text{Molar}}]_{\lambda,n,\text{Exp}}$ values should correlate strictly linearly with n . The quality of this correlation at four wavelengths is seen in Figure 10. A quantitative test of linearity is provided by linear length regressions applied to $[\theta]_{\text{Molar}}]_{\lambda,n,\text{Exp}}$ data sets from which the shorter Ala_n lengths are deleted. If core convergence is valid, the assigned slopes must be invariant. At 222 nm, the linear regression of the full data set yields a slope: $-59\,600$ (SD 1300), and an intercept: $202\,000$ (SD 20 700); if the first two data points are deleted (data set: $11 \leq n \leq 24$), the slope is $-59\,300$ (SD 1700); further restriction (data set: $14 \leq n \leq 24$) yields a slope of $-58\,800$ (SD 3100). Within standard error, these assignments are identical, and no deviations from linearity are detected at either low or high length limits.

Slopes for these regressions can be equated with $[\theta]_{\lambda,\infty}$, and these values are plotted in Figure 11. This is the first extrapolated

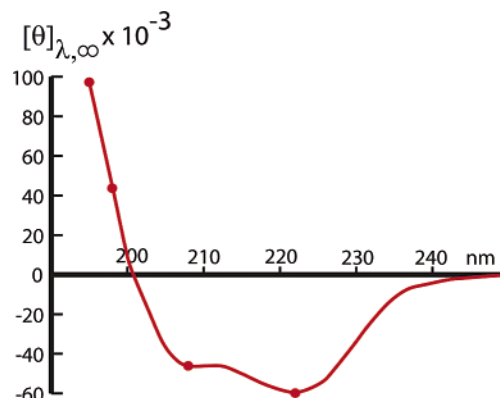


Figure 11. Extrapolated CD spectrum $[\theta]_{\lambda,\infty}$ of a completely helical Ala_n peptide in water at 2 °C. The red dots correspond to the slopes calculated from the linear length correlations of $[\theta]_{\text{Molar}}]_{\lambda,n}$ that appear in Figure 12. Units: $\text{deg cm}^2 \text{dmol}^{-1} \text{residue}^{-1}$. Except for the two regions within which $[\theta]_{\lambda,\infty}$ approaches 0, its least squares error is ca. 2% of its value.

CD spectrum of a fully helical alanine residue within the core region of a polyalanine helix, measured in water at 2 °C. The spectrum is qualitatively representative of benchmark literature spectra for limiting α -helices, but it is distinguished by the intensity of $[\theta]_{222,\infty}$ and by the ratio $[\theta]_{222,\infty}/[\theta]_{208,\infty} = 1.30$, larger than most literature values but consistent with our previous reports for alanine-rich peptides.^{12b}

To calculate both X and $[\theta]_{\lambda,\infty}$, we corrected series 3 $[\theta]_{\text{Molar}}]_{222,n}$ data for capping contributions by subtracting $[\theta]_{\text{Molar}}]_{222,0}$ values and dividing the resulting differences by the series of FH values listed in Table 1. In the normal process for calculating the FH of an n -residue peptide, eq 8, the experimental $[\theta]_{222,n,\text{Exp}}$ value is divided by $[\theta]_{\text{Molar}}]_{222,n}$, calculated by applying literature values of X and $[\theta]_{222,\infty}$ to eq 1. This process is reversed to calibrate X and $[\theta]_{222,\infty}$ from corrected molar ellipticities. Three linear length regressions were carried out using the low error limits, the mean values, and the high error limits of FH. Resulting values for $[\theta]_{222,\infty}$ are $-61\,200$ (SD 1300), $-60\,500$ (SD 1250), and $-59\,800$ (SD 1200). Corresponding values for X are 2.6 ± 0.3 , 2.8 ± 0.3 , and 2.9 ± 0.3 . Similar results are obtained if both series 2 and series 3 peptides are included.⁴⁹

Values of $[\theta]_{208,\infty}$ are also relevant to FH calculations. Linear length regressions of the corrected $[\theta]_{\text{Molar}}]_{208,n,\text{Exp}}$ data set yield values for $[\theta]_{208,\infty}$ of $-46\,000 \text{deg cm}^2 \text{dmol}^{-1}$ with X in the range 4.3–5.1. Notably, this $[\theta]_{208,\infty}$ lies close to the range of literature values.

Discussion

How general are the results of this study, which has been directed at clarifying problems with assigning NMR parameters and CD-based FH values to polyalanines and by analogy to alanine-rich peptides? The value of $[\theta]_{222,\infty}$, water 2 °C, assigned in this report, is 40% more intense than the upper limit of current literature values,^{34,46} which fall in the range -37×10^3 to $-44 \times 10^3 \text{deg cm}^2 \text{dmol}^{-1} \text{residue}^{-1}$. For typical helical peptide fragments derived from globular proteins, this range remains appropriate, but it is almost certainly underestimates $[\theta]_{222,\infty}$ for that class of helically disposed peptides that exhibit a ratio

(49) Least squares linear length regressions of combined, corrected series 2 and series 3 $[\theta]_{\text{Molar}}]_{222,n}$ data resulted in a ca. 2% decrease in $[\theta]_{222,\infty}$ and a 20% decrease in X .

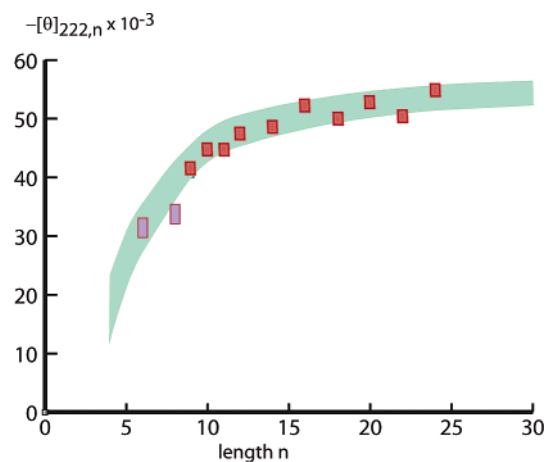


Figure 12. Green region graphs the length dependence of $[\theta]_{222,n}$, eq 1, calculated from $[\theta]_{222,\infty} = -60\,500$ (SD 1250) $\text{deg cm}^2 \text{dm}^{-1} \text{residue}^{-1}$ and $X = 2.8 \pm 0.3$ residues. Values of the 10 experimental ($[\theta_{\text{Molar}}]_{222,n} - [\theta_{\text{Molar}}]_{222,0}$)/FH values used to assign X and $[\theta]_{222,\infty}$ are plotted (red); for comparison, two corresponding values calculated from $[\theta_{\text{Molar}}]_{222,n}$, $n = 6$ and 8 are also shown (violet).

$[\theta]_{222}/[\theta]_{208}$ greater than 1.2 and curved parametric $[\theta]_{222}$ vs $[\theta]_{208}$ plots.^{12b} These include polyalanines and alanine-rich peptides. For these, our new $[\theta]_{222,\infty}$ value of $-60\,500 \pm 1300$ is the appropriate choice.

Figure 12 shows the calibration curve that results if the parameters derived in the preceding section are applied to eq 1. The large uncertainties in X generate correspondingly large errors in $[\theta]_{222,n}$ and FH. For a peptide of 24 residues the error in $[\theta]_{222,24}$ is $\pm 4\%$, but if the length is halved the error increases to $\pm 7\%$. Is there a need to calibrate helicity for short peptides? Peptides in the length range of 5 to 12 residues have been reported to exhibit weak CD spectra with helical features.⁵⁰ Recently reported examples include short, lanthanide cation-stabilized helical polyalanines.⁵¹ Figure 12 provides needed “ball park” estimates of limiting $[\theta]_{222,n}$ values for short peptides.

Can one improve the precision of X assignments for water-solubilized peptides? Unlike $[\theta]_{\lambda,\infty}$, which is defined largely by the CD properties of medium to long helical peptides, the X assignment must be based on experimental $[\theta_{\text{Molar}}]_{\lambda,n}$ data for short peptides. These data have intrinsically problematic features. Large assignment errors attend their weak ellipticities, and these are compounded by length uncertainties.

Since X reflects local effects of N- and C-caps, it must ideally be tailored to the particular capping structure of each new peptide series. The value of X is likely to depend on the nature of the polar atoms or charges that appear within end regions, which can influence N- and C-terminal conformations. The contribution of 3_{10} helical conformers to helical peptides of short to medium length⁵² poses a further ambiguity, since $[\theta]_{222}$ is weak for 3_{10} helices,⁵³ and variations in the $\alpha/3_{10}$ ratio are poorly understood.

- (50) (a) Zerkowski, J. A.; Powers, E. T.; Kemp, D. S. *J. Am. Chem. Soc.* **1997**, *119*, 1153–1154. (b) Gallo, E. A.; Gellman, S. A. *J. Am. Chem. Soc.* **1994**, *116*, 11560–11561. (c) Karle, I. L.; Balaram, P. *Biochemistry* **1990**, *29*, 6747–6756. (d) Parthasarathy, R.; Chaturvedi, S.; Go, K. *Proc. Natl. Acad. Sci. U.S.A.* **1990**, *87*, 971–875.
- (51) (a) Siedlecka, M.; Goch, G.; Ejchart, A.; Sticht, H.; Bierzynski, A. *Proc. Natl. Acad. Sci. U.S.A.* **1999**, *96*, 905–908. (b) Chin, D.-H.; Woody, R. W.; Rohl, C. A.; Baldwin, R. L. *Proc. Natl. Acad. Sci. U.S.A.* **2002**, *99*, 15416–15421.
- (52) (a) Miick, S. M.; Martinez, G. V.; Fiori, W. R.; Todd, A. P.; Millhauser, G. L. *Nature* **1992**, *359*, 763–655. (b) Long, H. W.; Tyko, R. *J. Am. Chem. Soc.* **1998**, *120*, 7039–7048.

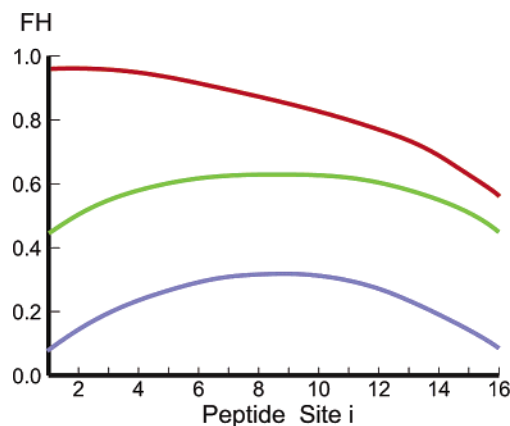


Figure 13. Lifson–Roig modeled⁸ FH values for a 16-residue homopeptide assigned a helical propensity w of 1.2. Blue curve: site-dependent FH values calculated for N- and C-terminal capping parameters of 1.0. Green curve: results of increasing capping parameters to 7.0. Red curve: N-capping parameter of 200; C-capping parameter of 7.

Why have we failed to detect 3_{10} structure for our series 2 N- and C-capped Ala_{*n*} peptides? The strong bias toward α -structure provided by the three preorganized hydrogen bonding sites of the β AspHel N-cap is a likely answer. Can the observed examples of 3_{10} structure seen with peptides derived from simple amino acids result from the reduced hydrogen bonding potential of water molecules or other functions available at helix ends? The presence of only two unsatisfied N-terminal NH hydrogen bonding valences for the 3_{10} helix may reduce its sensitivity to these factors.

Lifson–Roig modeling⁸ provides insight into the magnitudes of the helix-inducing capping effects we have observed in this study. The blue curve of Figure 13 demonstrates typical FH_{*i*} values for a medium-sized helically disposed homopeptide that lacks stabilizing N- and C-caps. Conformational averaging or “fraying” is responsible for the marked decrease of FH_{*i*} that is evident in the end regions.

The green curve results from a recalculation that introduces stabilizing N- and C-capping effects. A marked increase in FH_{*i*} is seen which is largest at the ends. A leveling is evident in the central region. Both effects are attributable to an increase in the mole fractions of substantially helical conformations. The red curve shows the effect of retaining a moderately stabilizing C-cap and introducing a highly stabilizing N-cap. The asymmetric site dependence of FH_{*i*} now shows little or no hint of fraying at the N-terminus. We believe the parameters used in calculating the red curve are reasonable approximations to the capping properties of β AspHel and *beta*, yet this curve underestimates the FH values we have documented for the capped peptides of this study. A second essential requirement for achieving FH values close to 1.0 is the presence of an amino acid with a high helical propensity. We have demonstrated a substantial length increase of the helical propensity w of alanine for short to medium-sized polyalanines,^{5c} and subsequent studies show that w assumes large values for peptides containing 20 or more residues.⁵⁴ This length dependence contributes to conformational homogeneity and compensates for an expected decrease in cap efficiency as the helical length is extended.

- (53) Toniolo, C.; Polese, A.; Formaggio, F.; Crisma, M.; Kamphuis, J. *J. Am. Chem. Soc.* **1996**, *118*, 2744–2745.
- (54) Kennedy, R. J., Ph.D. Dissertation, MIT, February, 2004.

Our success with generating a tractable length series of polyalanines with exceptionally high helicity almost certainly guarantees extension of the concept to other peptide classes. Previously studied highly helical alanine-rich heteropeptides are obvious candidates, but work in several laboratories has also demonstrated that unnatural amino acids with straight aliphatic side chains can have helical propensities equivalent to that of alanine.⁵⁵ Provided aggregation can be inhibited by appropriate solubilization, these are obvious candidates for future study. A necessary condition for all such studies is proof that the currently available strongly helix-inducing N- and C-caps can function as efficiently for more general peptide series as they have for the polyalanines. A particularly important goal is improving the efficiency of helix-stabilizing C-caps.

As tools for molecular engineering, peptides that assume fixed conformations have seen relatively little application. Given their conformational homogeneity, the capped Ala_n peptides of this study may become an important exception. They provide versatile cylindrical structures with defined lengths that can be extended within wide limits. Almost certainly these constructs will find roles as substrates for further NMR characterization of water-soluble peptide helices that lack stabilization from tertiary structure. Conformational averaging has hitherto plagued interpretation of physical data measured for simple helical peptides in aqueous solvents, but as this study has shown, structurally relevant databases comprising chemical shifts and coupling constants can now be measured through isotopic labeling of peptides similar to those of Ala_n series 2.

The interpretation of CD spectra of helical peptides raises many unresolved issues. How good is the widely accepted approximation that side chain substituents do not influence CD ellipticity? New second-generation calibration standards should allow this question to be addressed rigorously. A particularly important issue concerns temperature effects. Although they are the formal equivalents of the familiar extinction coefficients of electronic molecular spectroscopy, $[\theta]$ values differ in that they have been reported as exhibiting significant temperature dependence that may reflect conformational changes. Without helical calibration standards, and without the support of parallel NMR studies, it is difficult to draw rigorous distinctions between ellipticity changes that define this effect and those attributable to helix melting. We have recently reported a pertinent curvature test, based on a parametric plot of $[\theta]_{222}$ vs $[\theta]_{208}$ data, and have concluded that $[\theta]_{222}$ values for alanine-rich peptides are probably exceptionally temperature sensitive.^{12b} Further studies can be envisaged that employ FH-calibrated ellipticity standards to identify features of amino acid composition and sequence that correlate with the large temperature dependence of $[\theta]_{222}$. The immediate goals of such studies are potentially within reach and work toward a deeper predictive understanding of the factors that influence ellipticities for helical peptides.

More ambitious goals can also be envisaged. CD spectroscopy remains the most convenient, efficient, and inexpensive tool for detecting and quantitating helical structure within polypeptides and proteins. One can hope that the scope of CD analysis of helical peptides can be expanded to include assignment and

interpretation of subtle conformational features of helical peptides that currently lie beyond its scope.

Summary

N- and C-capped polyalanines that lack helical stabilization through tertiary interactions can approximate single fully helical structures. Two series, with general structures 2 and 3, have been shown by AUC to be unaggregated in water. NMR experiments with series 2 peptides have characterized structure and energetics. Literature-precedented conformations of the β AspHel N-cap and the C-cap *beta* have been shown to interact and stabilize the first and the last helical loops of the Ala_n sequences. The fully ionized carboxyl function of the N-cap, pK_a 3.27, is required for maximum helical stability. Analysis of Ala PF_i values and chemical shifts of Ala resonances lead us to the conclusion that the properties of the capped, solubilized Ala_n peptides can be classified into N-cap, core, and C-cap regions. For Ala_n peptides with $n > 8$, the residue fractional helicities FH_i of the $n - 8$ core residues lie at or above 0.99. The NMR resonances assigned to the central alanine core region of length $n - 8$ exhibit convergent helical ¹HN and ¹³C chemical shift values. The measured ³J_{HNH α coupling constants for the core region of the Ala₁₂ peptide allows assignment of the backbone dihedral angle ϕ as -50.5° , and α -helical structure is proved by detection of ³hJ_{NC} scalar couplings. Core length-dependent linear regressions carried out on $[\theta_{\text{Molar}}]_{\lambda,n}$ values measured for series 2 and 3 with $n > 8$ residues over the wavelength range of $195 \text{ nm} \leq \lambda \leq 350 \text{ nm}$ yield slopes that define the ellipticity parameter $[\theta]_{\lambda,\infty}$. Collectively these define the first extrapolated CD spectrum of a fully helical alanine residue within the core region of a polyalanine helix, measured in water at 2 °C. The value assigned to $[\theta]_{222,\infty}$ in this study is $(-60.5 \pm 1.3) \times 10^3 \text{ deg cm}^2 \text{ dm}^{-1}$, confirming our previous approximate assignments.^{5,12a} The limiting ellipticity value $[\theta]_{208,\infty}$ assigned in this study at the 208 nm minimum is $(-46 \pm 2) \times 10^3 \text{ deg cm}^2 \text{ dm}^{-1}$, in approximate agreement with literature values.}

Experimental Section

Synthesis, Purification, and Characterization of Peptides. Peptides were synthesized on a 0.02–0.03 mole scale by automated continuous-flow solid-phase synthesis using a PE Biosystems Pioneer Peptide Synthesizer with standard 9-fluorenylmethyleneoxy-carbonyl (Fmoc/HATU) chemistry, and peptides were cleaved from the resin as reported previously.^{5,9} Purification was carried out on a Waters 2690 HPLC with auto-injector and 996 detector using YMC ODS-AQ 200 Å 4.5 × 150 mm² columns. Characterization tables of mass spectrometric data obtained on a Waters ZMD mass spectrometer and AUC data obtained on Beckman Optima XI-A centrifuge equipped with a six-channel cell in an An-60 Ti analytical rotor can be found in the Supporting Information. The published synthesis⁹ for Fmoc-Hel-OH from Cbz-Hel-OH was modified as follows: hydrogenation on Pd–C was carried out in EtOH for 24 h yielding 94% of H-Hel-OH, which was transformed into Fmoc-Hel-OH, 71%, by prior esterification with TMS-Cl, reaction with Fmoc-Cl, and hydrolysis, following the procedure of Bolin et al.⁵⁶ The *N*-Fmoc-*trans*-4-aminocyclohexane carboxylic acid, Fmoc-Acc-OH, required for synthesis of peptides of series 2 was prepared by reaction of *trans*-4-aminocyclohexane carboxylic acid with Fmoc-Cl in aqueous buffer. Details of preparation and characterization

(55) (a) Lyu, P. C.; Sherman, J. C.; Chen, A.; Kallenbach, N. R. *Proc. Natl. Acad. Sci. U.S.A.* **1991**, *88*, 5317–5320. (b) Moreau, R.; Kemp, D. S. Unpublished observations.

(56) Bolin, D. R.; Sytwu, I.-I.; Humiec, F.; Meienhofer, J. *Int. J. Pept. Protein Res.* **1989**, *33*, 353–359.

of Fmoc-Acc-OH and preparation of Fmoc-Hel-OH can be found in the Supporting Information.

pH Assignments. Measurements were made at ambient temperatures in the pH range 1 to 9 with a Radiometer Copenhagen PHM240 pH meter equipped with a Cole-Parmer EW-55529-08 glass electrode, standardized daily with pH 4.0 and 7.0 standard buffers purchased from VWR Scientific. The rate measurements for amide NH \rightarrow ND exchange were conducted in D₂O; the pD meter readings were converted to pH values that are cited in the manuscript using the standard formula: pH = pD + 0.4.

CD Experiments. Circular dichroism measurements were obtained on an Aviv 62DS circular dichroism spectrometer as described previously.^{5,12b} The instrument was calibrated as described in the operating manual using previously titrated water solutions of sublimed 9-camphorsulfonic acid. Peptide concentrations were determined on a Cary 300 UV-vis spectrometer utilizing the Trp chromophore of the peptide, as previously reported.² From the deviations in linear length regression of $[\theta]_{222}$ in the region $12 < n < 19$ for the Ala_n series of Miller et al.,^{5b} the precision of $[\theta]$ is taken to lie in the range 3% to 5%.

NMR Experiments. All spectra were collected on a Bruker Avance 600 instrument (Karlsruhe, Germany) equipped with four channels and a pulsed field gradient triple probe with z gradients. Processing and data analysis were carried out on a SGI O2 workstation using XWINNMR 3.5 software (Bruker). Unless stated differently, all spectra except those for the NH-ND exchange experiments were obtained in H₂O/D₂O (95/5, v/v), 40 mM phosphate buffer, and spectra were measured with a relaxation delay of 1.8 s or greater. As noted below, the pH was adjusted as necessary by addition of small amounts of NaOH or H₃PO₄. DSS was used as an internal reference for ¹H chemical shifts, and ¹³C and ¹⁵N chemical shifts were referenced indirectly in accord with IUPAC recommendations.⁵⁷ For data processing in the indirect dimensions, zero filling was applied, and a square sine bell shifted by $\pi/2$ was used for apodization in all dimensions.

Studies of the (te) and (cs) Conformations of Ac ^{β} AspHel-Ala₈-beta-NH₂ Peptide 1. A 1D ¹H NMR spectrum was measured followed by standard TOCSY⁵⁸ (512c*4096c, τ_m = 70 ms) and ROESY⁵⁹ (512c*4096c, τ_m = 300 ms) spectra with sweep widths of 6613.76 Hz in both dimensions, using presaturation for solvent suppression. From these spectra, all chemical shifts were assigned as reported in the text, and a listing appears in the Supporting Information. To assign the pH dependences of resonances, a series of pH-dependent 1D ¹H spectra (16384c, sweep width 8992.0 Hz, pH range 1.3–8) were measured for a sample of peptide **1** containing uniformly ²H-labeled Ala residues. As reported in the text, significant pH dependences were only observed for the chemical shifts of three NH resonances.

A second, minor conformation could be detected in some spectra that showed a distinctive chemical shift of the C-12 resonance, linked by a cross-peak with a 9-H Hel resonance; these are signature features of the previously characterized (cs) state of a Hel-peptide conjugate.²⁰ The eight Ala NH resonances of the minor conformation were identified by their TOCSY signatures; they appeared downfield of resonances for the major conformation, implying weaker helicity. The resonance intensities of resonances associated with the (cs) conformation increase with an increase in temperature and decrease with an increase in pH or the length of Ala_n. At pH values below 3.8 and for the Ala-deuterated peptide, the (cs) state is sufficiently abundant to allow t/c to be estimated as a ratio of intensities of the Hel 12-H (t) and (c) proton resonances.⁶⁰ At pH 3.8, a value of 6 was observed at 320 K, which increased nearly linearly to a value near 12 as the temperature was decreased to 280 K.

Resonance intensities were measured for baseline-corrected 1D ¹H spectra (16384c, sweep width 8992.9 Hz, presaturated for solvent suppression) using the integration menu of XWINNMR. For the series **2** Ala₈ peptide uniformly labeled with ¹³C and ¹⁵N (see below), a 2D version H(N)CO of a standard HNCO experiment²⁸ in water at 8 °C, pH 4.5 yielded cross-peaks that correlate ¹³C=O chemical shifts for a site i Ala residues with ¹HN chemical shifts at the site $i + 1$. In addition to the cross-peaks expected for the major resonance, this experiment also showed much weaker cross-peaks for the minor resonances in the ¹³C=O chemical shift range 177.9–178.5 ppm, characteristic of random coil values. An approximate integration ratio gave values in the range 40–70 for t/c measured with an Ala₈ peptide under these conditions.

Studies of Ac ^{β} AspHelAla_nbetaAccLys₂TrpNH₂ n even, 8–16; Peptide Series 2. Assignment of the Ala ¹H HN resonances was carried out on each member of the series in the pH range 3.45–5.34 from standard TOCSY (512c*4096c, τ_m = 70 ms) and NOESY⁶¹ spectra (512c*4096c, τ_m = 400 ms) using a sweep width of 7183.9 Hz in both dimensions and watergate solvent suppression.

E.COSY HNCA and H(N)CO Experiments with Ac ^{β} AspHelAla₈-betaAccLys₂TrpNH₂ and Ac ^{β} AspHelAla₁₂betaAccLys₂TrpNH₂ Containing Uniformly ¹³C and ¹⁵N Labeled Ala Residues. Eight residues of the Ala₈ peptide were doubly labeled, but to minimize resonance overlap, Ala₁₂ peptides were synthesized in which labeling was confined either to residues 1–6 or to residues 7–12. The ¹³C α chemical shifts were assigned from a standard HNCA experiment, and the ³J_{H_NH α coupling constants were assigned from an E.COSY HNCA experiment (2048c*4c*64c). The sweep widths for both experiments were 5387.5, 426, and 1207 Hz respectively for the ¹H, ¹³C, and ¹⁵N dimensions. The values for the ¹³C α chemical shifts are shown in Figure 7a,b.}

For the two labeled Ala₁₂ peptides the ¹³C=O chemical shifts were assigned from a 2D version, H(N)CO, of a standard HNCO experiment²⁸ (1024c*256c) with a sweep width of 5387 and 980 Hz, respectively, for the ¹H and ¹³C dimensions. For the Ala₁₂ peptide with the last six Ala residues labeled, the nitrogen to carbonyl dephasing time ($2T$) was set to 0.024 s, which corresponds to a value of slightly shorter than $1/(2*^1J_{\text{NCO}})$, ¹J_{NCO} = 15 Hz, a commonly used value for correlations of chemical shift values for a residue i , ¹³C=O with residue $i + 1$ ¹HN. For the hydrogen bonding experiment,³² data were measured at 10 °C in 40 mM phosphate buffer, pH 4.46, at a sample concentration of 2–4 mM in a Shigemi NMR tube (Tokyo, Japan) on the Bruker spectrometer, equipped with a ¹H, ¹³C, ¹⁵N triple resonance 5 mm CryoProbe. A data matrix of 2048c*32c was collected with a sweep width of 3894 and 203.7 Hz for the respective ¹H and ¹³C dimensions. The hydrogen bonding spectrum of the C-terminally labeled peptide, Figure 7b, was measured with $2T = 0.1316$ and 512 scans, which allows detection of ³J_{N_C scalar couplings.³² Similar measurements were carried out on the labeled Ala₈ peptide and the N-terminally labeled Ala₁₂ peptide, Figure 7a. The spectrum of Figure 7c was measured with $2T = 0.1303$ and 1024 scans, and data from this experiment were used to calculate signal-to-noise values.}

Protection Factor Measurements on Peptides of Series 2 and 3.

A PF _{i} value for base-catalyzed amide NH \rightarrow ND exchange in D₂O is the ratio of the second-order rate constant $k_{2\text{NHsid}}$ measured for a model unstructured amide NH and the analogous rate constant $k_{2\text{PeptideNH}_i}$ measured under the same conditions for a backbone NH at site i of a test alanine peptide. Values reported by Bai et al.¹¹ for pH and temperature dependence of $k_{2\text{NHsid}}$ were used in this study and independently confirmed.⁶² Amide proton-deuterium exchange experiments were conducted at 2 °C in D₂O (20 mM phosphate buffer) containing 1–2 mM peptide samples; the pD measurements for these experiments were converted to the reported pH values with the standard equation: pH = pD + 0.4. An optimal pH for NH \rightarrow ND exchange

(57) Markley, J. L.; Bax, A.; Arata, Y.; Hilbers, C. W.; Kaptein, R.; Sykes, B. D.; Wright, P. E.; Wüthrich, K. *Pure Appl. Chem.* **1998**, *70*, 117–142.

(58) (a) Bax, A.; Davis, D. G. *J. Magn. Reson.* **1985**, *65*, 355–360. (b) Braunschweiler, L.; Ernst, R. R. *J. Magn. Reson.* **1983**, *53*, 521–528.

(59) Bax, A.; Davis, D. G. *J. Magn. Reson.* **1985**, *65*, 207–213.

(60) Kemp, D. S.; Curran, T. P.; Boyd, J. G.; Allen, T. J. *J. Org. Chem.* **1991**, *56*, 6672–6682.

(61) Jeener, J.; Meier, B. H.; Bachmann, P.; Ernst, R. R. *J. Chem. Phys.* **1979**, *71*, 4546–4553.

(62) Kennedy, R. J.; Kemp, D. S. Unpublished observations.

for all alanine NH resonances was found to lie in the range 4.5–4.8, which ensured that the β AspHel helix-inducing cap was maximally effective and allowed convenient measurement of the slow exchanges observed for the core alanine NH functions. Time-dependent peak heights and curve-fitted resonance areas for ^1HN NMR resonances were carried out for both series **2** and series **3** peptides and found to be in reasonable agreement; satisfactory fits to pseudo-first-order behavior were observed over at least three half-lives. Curve fitting was performed using the spreadsheet and graphing software package Origin. The NMR spectra were fit with Lorentzian peaks through the Fit Multi-Peaks option from the Analysis menu. Each identifiable peak was fitted with a single Lorentzian peak; thus, for the longer peptides, the core alanine residues were fitted with a single peak. The R^2 values for the fits were typically greater than 0.99; the lowest value observed was 0.96. All fitted peaks had appropriate line widths for amide protons. Owing to its rapid $\text{NH} \rightarrow \text{ND}$ exchange at a $\text{pH} > 4.5$, upper and lower limits for the PF_{n+1} value for the NH of *beta* were assigned by estimating for an Ala₈ peptide the relative pH dependence of the NH resonance broadening in H₂O in the pH region where intermediate line broadening due to proton exchange is observed. These were compared with values

for a *beta*-containing random coil model to estimate likely upper and lower bounds for PF_{n+1} .⁶³ Calibration with Ala NHs showed satisfactory consistency with PF values measured above.

Acknowledgment. Financial support was provided by NSF Grant CHE-0131250 (G.E.J. and B.H.), by NIH Grant GM13453 (S.M.W. and R.J.K.), and by Pfizer Research. We also thank the NIH for funding through Grant 1S10RR13886-01 that allowed purchase of the Bruker CryoProbe, located in the MIT Chemistry Department Spectroscopy Laboratory.

Supporting Information Available: An appendix of equation justifications and calculation derivations, synthetic details for key intermediates, peptide NMR and MS characterization tables, and AUC data. This material is available free of charge via the Internet at <http://pubs.acs.org>.

JA0457462

(63) For a precedent applied to fast equilibration of ^{13}C resonances, see: Park, S.-H.; Shalongo, W.; Stellwagen, E. *Proteins: Struct., Funct., Genet.* **1998**, *33*, 167–178.